Transcriptomic and functional characterization indicate sexual dimorphism of discrete circadian neuron subtypes

Pérez Torres, Melina[1] ; Jiang, Ruihan[2,3] ; Ma, Dingbang[1,4]; Kurmangaliyev, Yerbol[1]; Guo, Fang[2,3] ; Rosbash, Michael[1]*

1 Howard Hughes Medical Institute and Department of Biology, Brandeis University, Waltham MA, 02452, USA

2 NHC and CAMS Key Laboratory of Medical Neurobiology, Zhejiang University School of Medicine, Hangzhou 310058, China.

3 Department of Neurobiology, Department of Neurology of Sir Run Run Shaw Hospital and School of Brain Science and Brain Medicine, Zhejiang University School of Medicine, Hangzhou 310058, China

4 Interdisciplinary Research Center on Biology and Chemistry, Shanghai Institute of Organic Chemistry, Hi-Tech Park, Pudong, Shanghai 201210, China

* To whom correspondence should be addressed: MR

Abstract

Many sexually dimorphic behaviors exhibit a time-of-day preference, but our understanding of how sex shapes the molecular and circuit properties of central brain neurons remains incomplete. Here, we report a transcriptomic and circuit underpinning of sexual dimorphism within the *Drosophila* circadian network. By performing single-cell RNA sequencing of male and female clock neurons, we identify specific subsets of dorsal lateral neurons (LNds), dorsal neurons 1p (DN1ps) and dorsal neurons 3 (DN3s) with dramatic dimorphic gene expression profiles. These sex differences are driven in large part by cell-type-specific expression of genes involved in neural connectivity, particularly cell adhesion molecules (CAMs). We focused on the dimorphic Cry-negative E3 LNds and show that they form functionally active, synaptic connections with downstream *doublesex*-expressing pC1 and pCd neurons, central regulators of dimorphic behaviors. Moreover, we demonstrate that these connections are mediated at least in part by sex-enriched CAMs, dpr9 in males and dpr3 in females. Thus, our work reveals sexual differentiation mechanisms at both the molecular and circuit levels, identifying specific molecules that sculpt sex-specific pathways and link the circadian clock to dimorphic outputs.

Introduction

The study of circadian rhythms in *Drosophila* has historically focused on behaviors such as eclosion and locomotor activity, revealing a core transcription-translation feedback loop (TTFL) that governs these rhythmic behaviors (Allada et al., 1998; Blanchardon et al., 2001; Myers et al., 2003; Sheeba et al., 2008). There is however, a wide array of additional behaviors beyond these canonical outputs that also exhibit a time-of-day preference, which include male sex drive, female receptivity, oogenesis, and oviposition. Moreover, central brain circadian neurons as well as components of the TTFL are implicated in regulating these sexually dimorphic behaviors (Sakai & Ishida, 2001; Manjunatha et al., 2008; Fujii & Amrein, 2010; Fujii et al., 2017; C. Zhang et al., 2021).

At the heart of this regulation is the circadian network, a circuit of approximately 240 neurons anatomically classified into seven groups: dorsal neurons (DNs-- divided into DN1a, DN1p, DN2, DN3), dorsal lateral neurons (LNds), ventral lateral neurons (LNvs) and lateral posterior neurons (LPNs) (Reinhard et al., 2024). Decades of research have identified specific roles for many of these anatomical clusters. For example, the LNvs (also known as M cells) are the master regulators of morning anticipatory locomotor activity and rhythmic activity in constant conditions such as constant darkness (Grima et al., 2004; Stoleru et al., 2004). The LNds or E cells are a group of six neurons per hemisphere subdivided into E1-E3, which display substantial heterogeneity in gene expression and neuron projections. E1 and E2 LNds encompass four Cry-expressing neurons, which have been studied for their roles in regulating evening anticipatory behavior and sexually dimorphic behaviors (Hamasaka et al., 2010; Grima et al., 2004; Stoleru et al., 2004; Shafer et al., 2022; Brown et al., 2024; Le et al., 2024; Kim et al.,

2012, 2013). The remaining LNds are the E3s, which consist of the three Cry-negative LNd neurons per brain hemisphere; they have been less studied due to minimal connections between them and the rest of the circadian circuit (Shafer et al., 2022). The LPNs have been found to regulate daily activity/rest patterns in response to environmental temperature fluctuations. The DN1 neurons are a heterogeneous population involved in sleep regulation and time-of-day perception (Guo et al., 2016; Poe et al., 2023). The DN2 cells regulate temperature rhythm entrainment, and the DN3s are sleep-promoting neurons (Picot et al., 2009; Sun et al., 2022; Ma et al., 2025).

Recent advances in single-cell RNA sequencing (scRNA-seq) have revealed a new layer of complexity within circadian neurons, identifying at least 27 transcriptionally unique circadian clusters. This transcriptional heterogeneity splits the anatomically assigned cell types into multiple sub-clusters. These clusters were identified by the expression of previously defined cell-type-specific features such as neuropeptides, GPCRs, and cell adhesion molecules (CAMs) expression. Interestingly, CAMs alone are sufficient to define the circadian clusters, suggesting highly cell-type-specific expression of these connectivity molecules (Ma et al., 2021, 2023, 2025).

Such neural connectivity molecules carry out essential roles in neuronal communication and wiring specificity throughout development (Hewes & Taghert, 2001; Hauser, 2006; Engle, 2010; Jeong, 2021; Schlichting et al., 2022; Ma et al., 2023). Several of these molecules have been implicated in the regulation of sexually dimorphic neuronal connectivity, such as members of the *roundabout* (*robo*) and *defective proboscis extension* (*dpr*) CAMs (Goldman & Arbeitman, 2007; Mellert et al., 2010b; Brovero et al., 2021). The expression of some CAMs is modulated by one of the master regulators of

sexually dimorphic outputs, *fruitless* (*fru*). Examples include *dpr* and its connecting partner *dpr-interacting partner* (*dpr*/*DIP*); their expression within the fly brain identified sexual differences in cell number and neuron morphology (Brovero et al., 2021). Multiple FruM binding sites were found in or near *dpr*/*DIP* genes, suggesting that these molecules are regulated by *fru* (Brovero et al., 2021). FruM-specific accessible chromatin regions are more generally found near axon guidance and CAMs, potentially acting as sex-specific regulatory elements (Brovkina et al., 2021).

The fly brain contains multiple clusters containing sexually dimorphic neurons. They regulate dimorphic behaviors and are characterized by sex-specific *doublesex* (*dsx*) and *fru* isoform expression (Ito et al., 1996; Villella & Hall, 1996; Rideout et al., 2010). Among these clusters are the P1/pC1 neurons in males and pC1 in females. They are multisensory integrators of environmental cues and are necessary for successful mating, i.e. these neurons receive chemical and auditory stimuli to carry out sexually dimorphic behavioral outputs such as courtship and mate receptivity. P1/pC1 neurons interact with pCd neurons, which maintain persistent behavioral states elicited by male P1 neurons (Zhang et al., 2016; Jung et al., 2020). In females, pCd neurons respond to male-specific pheromones to modulate mate receptivity (Deutsch et al., 2020). The time-of-day preference of several dimorphic behaviors suggests interactions between the circadian neurons and the dimorphic circuitry. However, the nature of these interactions and the role of sexually dimorphic gene expression within circadian neurons have remained largely unexplored.

We therefore began this study by investigating the transcriptional profile of circadian neurons with a focus on sexually dimorphic gene expression. By performing

single-cell RNA sequencing of male and female circadian neurons, we identified subsets of LNds, DN3s, and DN1p neurons with sexually dimorphic differences, which are enriched for genes impacting neural connectivity: CAMs, GPCRs, and neuropeptides. One sexually dimorphic circadian subgroup is the LNds, which are upstream of and connect to the *dsx*-expressing pC1 and pCd neuronal subsets. We further demonstrate that this connection is mediated at least in part by sex-specific CAMs expressed within the LNds. Lastly, these neurons require *fru* expression to regulate locomotor activity behavior in male flies but not in females, indicating a sexually dimorphic role for these LNds in regulating sex-specific behaviors.

Results

Four circadian cell types show a sexually dimorphic transcriptomic profile

Recent studies from our lab used single-cell RNA sequencing to characterize the transcriptomes of circadian neurons and demonstrated that they could be clustered into at least 27 distinct cell types (Ma et al., 2021, 2023, 2025). Because previous studies have reported that there are sexually dimorphic cell types within the circadian neuronal circuit (Hanafusa et al., 2013; Palmateer et al., 2023; Deluca et al., 2024). we re-examined these neurons using single-cell sequencing libraries prepared from either male or female circadian neurons (Fig. 1A).

To this end, male or female flies expressing an enhanced GFP (eGFP) fluorescent marker in all circadian neurons (*Clk856-Gal4, DN3-spGal4, UAS-eGFP*) were collected at ZT06 and ZT18. Brains were dissected, and GFP-positive neurons were isolated using a fluorescence-activated cell sorter (FACS). Single-cell transcriptomic profiles of male and female clock neurons were generated using 10X Genomics (see Methods). The male and female data sets, 2,451 male and 2,865 female cells (Fig. 1B), were integrated (referred to as the “sex-informed” data set), and 2000 variable features were used for principal component analysis (PCA) and cluster generation. We clustered this dataset *de novo* and showed that it strongly correlated with our previous single-cell sequencing studies of clock neurons (Fig. S1A; Ma et al., 2025). By examining the distribution of male and female neurons, we found several cell types in which male and female transcriptomes were sufficiently different to split these neurons into two clusters, or a single cluster was subdivided by sex (Fig. 1C, circled in dashed green; blue is male, and pink is female).

These data indicate that at least a cluster of LNds and two DN3 circadian cell types show sexually dimorphic gene expression patterns.

Previous studies have used the expression of sex-specific transcripts to validate sex-derived cells in single-cell data sets (Palmateer et al., 2023; Epiney et al., 2025). To test whether this approach would provide a complementary approach for *Drosophila* circadian neurons, we examined the expression of several sex-specific genes (Fig. 1D; Fig. S1B-D). The male-specific non-coding RNA *roX1* was most useful and detected in 48% of cells; male-derived cells exhibit higher *roX1* transcript levels, whereas female-derived cells show low or undetectable *roX1* expression (Fig. 1D; Fig. S1E-F). Using the Receiver Operating Characteristic (ROC) as a performance metric for true and false positive rates, we identified high correlation (AUROC= 0.998) between *roX1* expression levels and male sex-assignment. This analysis determined that the optimal cutoff for sex assignment was 9.4 normalized counts (2.3 log1p-normalized expression) (Fig. S1G).

To increase statistical power and ensure sufficient coverage of smaller circadian cell types, an additional circadian neuron transcriptomic data set was generated and combined with the above sex-informed dataset and a previously published circadian single-cell dataset (see Materials and Methods, Fig. 1E, Fig. S2-S4; Ma et al., 2025). This final data set consists of 22,306 high-confidence circadian neurons from both sexes. To infer sex in this data set, we used the sex-assignment cutoffs described above, normalized *roX1* counts greater than 10 define male cells and counts less than 2.3 define female cells; this inferred data set contains 11,434 male cells and 10,872 female cells (Fig. 1F-G). Its sex distribution confirms the transcriptomic profiles described above (Fig.S2A-B). This comprehensive analysis clarified a key point: two previous distinct

circadian LNd clusters/cell types (9:LNd_NPF/12:LNd_AstC, also known as LNd_1/LNd_2) are in fact the same cell type separated by sex. Marker gene expression analysis of this sexually dimorphic cell type indicates that these are the understudied E3 LNds (named LNd_c in the FlyWire EM connectome). We also identified two closely related DN3 clusters (DN3-9a/d and DN3-9c/b) and one subset of DN1ps (DN1p-4) with dramatic sex-biased transcriptional clustering.

There are also differences in the number of male and female circadian neurons in the LNds, DN1s, and DN3s. The ratio of male-to-female cells within each cluster was calculated from the sex-inferred dataset, where male and female cells were processed together (Fig. S2C). This dataset does not have a bias in cell number due to possible differences in cell recovery like the sex-informed data set. The dimorphic DN3 cluster (DN3-9a/d) shows three times more male cells than female cells, whereas its transcriptionally related DN3-9c/b cluster shows equal numbers of male and female cells. This observation is consistent with a recent study reporting more DN3s in male adult brains than in females (Deluca et al., 2024). The LNd clusters (LNd-1 and LNd-2) show 1.6X more male neurons than female neurons (Fig S2C); previous anatomical studies of the lateral clock neurons consistently describe approximately six LNd neurons per hemisphere and do not report sex differences in LNd cell numbers (Helfrich-Förster, Shafer, et al., 2007; Helfrich-Förster, Yoshii, et al., 2007; Schubert et al., 2018). Additionally, several DN1p transcriptional clusters show between 1.1X and 1.3X more male clock neurons, consistent with previous reports identifying sexual dimorphism in *fruitless* (*fru*)-expressing DN1p cell types (Fujii & Amrein, 2010; Hanafusa et al., 2013). The sex-biased cell numbers appear specific for these circadian clusters as the non-

sexually dimorphic cell types show similar if not identical numbers of male and female circadian neurons (Fig. S2C).

Sex-Differentiated Gene Expression in Circadian Clusters is Cell-Type-Specific

To identify the molecular underpinnings of this dimorphism, we searched for marker gene expression that defines the different circadian clusters. *fru* is upregulated in these four sex-biased clusters; *fru* expression has been previously reported in a small subset of DN1s and LNds (Fig. S5A; Palmateer et al., 2023). The two sex-biased DN3 clusters also express *zelda* (*zld*), a transcription factor involved in sex determination (Fig. S5B). Moreover, a defining feature of the male LNd cluster (LNd-1) is the *neuropeptide F* (*NPF*, Fig. S5C); previous work identified NPF as sexually dimorphic (Lee et al., 2006).

To further characterize sexually dimorphic features within this data set, differential gene expression analysis was performed between male and female cells from each circadian cluster. Most clusters have fewer than 10 sex-differentially expressed genes, whereas four clusters show more substantial differential gene expression (Using an adjusted p-value cutoff of less than 0.05 and fold change cutoff of 1.7 or greater; Fig. 2A). The LNd clusters show 42 male-specific genes and 19 female-specific genes. The two DN3 clusters (DN3-9bc and DN3-9ad) have 35 and 33 male-specific genes, whereas females have 32 and 31 female-specific genes, respectively. Lastly, the one sexually dimorphic DN1p cluster (DN1p-4) has 12 male and 17 female-specific genes (Tables 1 and 2). There are few overlapping sex-specific genes; the high degree of cell type-specificity suggests that these genes and neurons regulate distinct aspects of sexually dimorphic outputs (Fig. 2B-C).

As expected, *lncRNA:roX1* and *lncRNA:roX2* are exceptions and commonly upregulated in all male cells (Franke & Baker, 1999; Meller & Rattner, 2002). *sister-of-sex-lethal* (*ssx*) is also significantly upregulated in several subsets of male neurons; *ssx* is known to promote male-specific features (Moschall et al., 2019). Two additional novel sex-specific genes are encoded on the X chromosome: *Muc14a* is upregulated in nine male dorsal neurons, and *terribly reduced ocelli* (*trol*) is upregulated in male cells from three DN1p and DN2 clusters (Fig. 2B, Table 1).

The most common female-enriched gene is *Sex lethal* (*Sxl*), the primary feminizing switch during sex determination (Bell et al., 1991). Interestingly, the *pigment-dispersing factor receptor* (*Pdfr*) is differentially upregulated in female LNvs, LNds, and DN3-9b; whole-body *Pdfr* mutants have sexually dimorphic behavioral differences (Iyer et al., 2024). Additional differentially expressed genes in female cells include *CG15765*, identified in a genome-wide association study (GWAS) as a candidate for modulating neural input affecting sperm competition in females (Chow et al., 2013). Other common upregulated genes in female circadian neurons have not been associated with sex-specific physiology or behavioral functions (*CG34247*, *alpha-Man-Ia*, *CG44422*, and *PVRAP*) (Fig. 2C, Table 2).

Sexually Dimorphic Circadian Clusters Are Enriched for Neural Connectivity Molecules

Because of the modest number of differentially expressed genes from individual clusters, gene ontology (GO) analysis was performed on the combined set of sex-differentiated genes from the top four dimorphic clusters for both sexes. This set of 101 male-enriched genes and 79 female-enriched genes were compared to a background of

3,741 genes detected in all circadian neurons. The top GO term in both sexes was the GPCR signaling pathway (GO:0007186), which includes both GPCRs and neuropeptides. Signaling, signal transduction and sensory perception of chemical stimuli were enriched GO groups for male-expressed genes. Female genes were enriched for cell-cell adhesion, CAMs, and signal transduction (Fig. 3A-B). These similar GO categories suggest similar and/or related sex-specific functions in both male and female clock neurons despite strong cell type-specific gene expression.

These GO categories and functions recall the fact that neural connectivity molecules are defining features of circadian cell types (Ma et al., 2023). Given that our GO analysis revealed common gene group enrichment, we investigated the specificity of neural connectivity molecules in our dataset. Neuropeptides, GPCRs, and CAMs are indeed differentially expressed by sex in the top four dimorphic clusters (Fig. 3C-E, Fig. S6A-B). The LNds show strong sexual dimorphic expression of *NPF* and *Proctolin* (*Proc*); *NPF* is enriched in male LNds, consistent with previous studies (Lee et al., 2006), whereas *Proc* is enriched in female LNds. Although *Proc* serves as a signaling factor important for oviposition in other cell types (Belanger & Orchard, 1993), this is the first report of its sexually dimorphic gene expression within circadian neurons. Three neuropeptides are dimorphically expressed in the DN3-9a/d cluster: *sNPF*, *Dh44,* and *CG33639*. Only *Dh44* has been reported to contribute to sex-specific behaviors in other cell types (Nässel & Zandawala, 2020).

Sexually differentiated GPCRs within the dimorphic circadian clusters include several receptors. Although they contribute to sexually dimorphic behaviors, including activity/rest periods, oogenesis, courtship, and mating (Guo et al., 2016; B. Ma et al.,

2022; Certel et al., 2010; C. Zhang et al., 2021; S. X. Zhang et al., 2016; Zhou et al., 2008; Crickmore & Vosshall, 2013), the function of these GPCRs in clock neurons is unknown. An exception is the expression of *mGluR* in subsets of LNds; it regulates the sexually dimorphic behavior of daytime activity (Guo et al., 2016). *mGluR* is upregulated in male LNds, but the same gene is also upregulated in both female DN3 dimorphic clusters (DN3-9b and DN3-9d). This suggests different roles of this GPCR in dimorphic outputs based on cell identity (Fig. 3C).

The largest number of sexually differentiated genes in the dimorphic clusters are CAMs, mainly belonging to the immunoglobulin superfamily (IgSF) of proteins; they include *defective proboscis extension* (*dpr*) and *Dpr-Interacting Partner* (*DIP*) as well as members of the *beaten Path* (*beat*) family of molecules that regulate axon guidance and cell-cell recognition. The LNd cluster has four male-enriched and one female-enriched *dpr genes*, of which the highest fold change differences were for *dpr9* in male LNds and *dpr3* in female LNds (Fig. 3E). Each DN3-9 clusters has two male enriched-genes; one (*dpr1*) is shared between these two male clusters and gates the timing of male courtship steps in other cell types (Goldman & Arbeitman, 2007), while the other, *dpr9*, is shared between male LNds and DN3-9c. Overall, we have identified sexually dimorphic neural connectivity molecules in subsets of circadian cell types where CAMs (35 genes) and GPCRs (12 genes) display an overrepresentation in each sex within circadian cell types.

Sex-Specific CAMs Mediate Functional Connectivity between LNds and Downstream Dimorphic Circuits

LNds have been associated with several sex-specific behaviors (Howlader & Sharma, 2006; Hamasaka et al., 2010; Kim et al., 2013; Riva et al., 2024), and these

neurons can be manipulated using the *DvPDF*-Gal4 transgenic driver. To address possible synaptic connectivity between LNds and *doublesex*-expressing (*dsx*) neurons known to regulate sexually dimorphic physiology and behavior (Rideout et al., 2010; Zhou et al., 2015; Jung et al., 2020; Wang et al., 2021), we used a modified version of the *trans*-synaptic labeling tool, *trans*-TANGO, to restrict postsynaptic labeling to neuronal subsets of interest (Talay et al., 2017). This restricted *trans*-TANGO uses a membrane-bound ligand expressed in axonal projections of presynaptic neurons and a ubiquitously expressed QS transcription factor flanked by FRT sites for conditional expression in specific candidate cells. The *DvPDF-Gal4* driver was used as the presynaptic driver where the *trans*-TANGO ligand is expressed, and postsynaptic target neurons were restricted to *dsx*-LexA-expressing neurons along with *LexAop-FLP* (Fig4A; Sun et al., 2022).

There was an average of 15 pCd and 25 pC1 neurons in male brains and an average of 10 pCd and 12 pC1 neurons in female brains postsynaptic to *DvPDF-Gal4*-expressing circadian neurons; this was based on neurite projection pattern and anatomical location (Fig. 4B-C). Restricted *trans*-TANGO validation used sparse LexA drivers to label discrete *dsx*-positive neuronal subsets; these data indicated that pC1 and pCd but not pC2 are directly downstream of *DvPDF-Gal4*-expressing neurons (Fig. 4E). Although there were only 1-3 labeled cells per hemisphere, these drivers might only label a fraction of the cells within their respective cell types (Zhou et al., 2014). Connectivity analysis using the FlyWire EM connectome (Dorkenwald et al., 2022) confirms that the E3 LNds (LNd_c) have direct input to pCd and pC1 subsets; the other *DvPDF-Gal4*-expressing neurons such as s-LNvs do not share this connection (Fig. 4D).

To test whether this anatomical linkage represents a functional circuit, we performed a series of optogenetic stimulation and calcium imaging experiments (Fig. 5A; Sun et al., 2022). Briefly, a red-light-activatable channelrhodopsin (UAS-CsChrimson-td-Tomato) was expressed under *DvPDF-Gal4* control, and *dsx*-LexA promoted the expression of a calcium indicator (LexAop-GCaMP6s) in the same flies. In both male and female brains, intermittent red-light stimulation of DvPDF-labeled neurons resulted in an increase in GCaMP signal from the cell body and projections of *dsx*-positive neurons (Fig. 5B-C), indicating that the circadian LNds have functional connections to *dsx*-positive pCd and pC1 neurons.

CAMs are known target of sex-specific isoforms of *fru* and have been found to drive sex-specific projection patterns of neurons (Yu et al., 2010; Cachero et al., 2010; Brovkina et al., 2021). We therefore asked whether *dpr9* and *dpr*3, the top differentiated CAMs in males and female LNds respectively, contributed to *dsx* circuit function. To this end, a similar experimental design as described above was used in combination with a knockdown of either *dpr3* or *dpr9* under *DvPDF-Gal4* control; GCaMP6s was recorded in both sexes from the cell body and projections of cells labeled by *dsx*-LexA (Fig. 5D).

Knockdown of the male-enriched CAM, *dpr9*, in male LNds resulted in a significant reduction of GCaMP signal from *dsx* neurons. In contrast, knocking down female-enriched *dpr3* in male cells resulted in a more modest (but still significant) decrease in Ca^{2+} influx (Fig. 5E). Similarly, knocking down the female-enriched CAM, *dpr3*, in female LNds resulted in a significant reduction in GCaMP signal, whereas the *dpr9* knockdown in female LNds had no effect, i.e., it had a comparable GCaMP signal to the control

condition (Fig. 5F). These results indicate that some LNd-sex-enriched CAMs help connect to downstream sexually differentiated neurons.

Lastly, we addressed the behavioral significance of these molecular and circuit-level findings by assaying mating activity after CRISPR-mediated knockout (KO) of several candidate LNd dimorphic genes including those described above. Somewhat to our surprise, there was no significant effect on mating, which included mating latency and mating duration (data not shown).

Discussion

The recent transcriptomic profiling of *Drosophila* clock neurons has unveiled dramatic transcriptional heterogeneity within the circadian circuit, far exceeding what anatomical classifications had suggested (Ma et al., 2025). However, these comprehensive transcriptomic maps ignored had the extent to which sex might drive transcriptomic differences. This possibility is also interesting because circadian neurons and clock-controlled genes are involved in a series of sexually dimorphic physiologies and behavior. For these reasons, we characterized sexual dimorphism of *Drosophila* clock neurons. The results include at least two clusters of DN3s, which are arguably the most enigmatic group of clock neurons (Ma et al., 2021, 2025; Helfrich-Förster et al., 2007b; Reinhard et al., 2024). There is also a sexually dimorphic group of LNds, which are the E3 LNds. They not only have highly sexually dimorphic transcriptomes, but they also connect to some of the central regulators of sexually dimorphic behaviors.

In our original transcriptomic profile of clock neurons (Ma et al., 2021, 2025), we identified two LNd clusters that we interpreted as distinct subtypes; however, our current

analysis shows that this subdivision reflects a single LNd subtype split by sex. In contrast, the remaining sexually dimorphic clusters observed in this study did not segregate in the original dataset. Several technical and biological factors may explain this discrepancy. First, the present work isolated clock neurons using an H2A-GFP fusion protein, which is stronger and more stable than the cytoplasmic eGFP reporter used previously. The current work may therefore have labeled a broader population of circadian neurons, increasing our ability to detect subtle transcriptomic differences in the adult brain. Second, the earlier dataset may have recovered relatively few neurons of each sex per time point, potentially limiting statistical power to resolve sex-specific transcriptional signatures. As a result, clusters that are now clearly dimorphic may have previously appeared as single, mixed-sex populations.

The hierarchical role of the LNds categorizes them as core activity-promoting neurons; the E1 and E2 LNds are important in different aspects of locomotor activity behavior (Shafer et al., 2022; Brown et al., 2024; Le et al., 2024). The E3 cells in contrast have no known role in these behaviors. Moreover, circadian connectivity analysis has identified only sparse interactions between the E3 LNds and the rest of the circadian circuitry, suggesting that these neurons might predominantly connect to neurons that are upstream or downstream of the clock neurons. For example, the E3 LNds might connect to inputs that help adapt the clock to temperature (Yoshii et al., 2010; Shafer et al., 2022). Additionally, studies have implicated the LNds in sexually dimorphic behaviors such as rival-induced mating duration, mating drive, and oviposition. However, the role of E3 LNds in these behaviors has not been previously studied despite evidence that the clock is

involved and that the expression of *per* and *tim* in circadian neurons is required for rival-induced long mating duration (LMD) (Kim et al., 2012).

A key question arises from our findings: since the E3 LNds are relatively isolated from communication to many other clock neurons but maintain robust connections with pC1 and pCd neurons in the adult, what messages are they relaying? Neuronal connectivity molecules (e.g., CAMs) are known to regulate wiring specificity. The binding affinity for the *dpr*/*DIP* partnership varies between interactions, which suggests variability in the strength of the synaptic connections that contribute to wiring (Carrillo et al., 2015; Zinn & Özkan, 2017). Although both male and female E3 LNds connect to pC1 and pCd neurons, the strength of this connection might be modulated by these sex-specific connectivity molecules in a sex- and context-dependent manner.

In *Drosophila*, the earliest detection of *fru* transcripts coincides with the first appearance of what are thought to be the circadian LNd and DN3 neuronal clusters. The sexual dimorphism of these neurons likely originates from the late stages of pupal development (Kaneko et al., 1997; Lee et al., 2000; Helfrich-Förster, Shafer, et al., 2007; Houl et al., 2008). It is possible that, as these *fru*-expressing neurons develop, sex-specific isoforms of FRU regulate the expression of sexually dimorphic connectivity molecules, which influence gene expression and developmental wiring in a sex-dependent manner. This could explain why the misregulation of genes involved in sexual differentiation results in altered locomotor activity behaviors in both sexes. Further, the reason we did not observe locomotor activity defects upon a *dpr* KO may be due to compensatory or redundant molecules that replace these *dprs* upon a KO. Another

possibility is that these molecules play a role in other sexually dimorphic behaviors yet to be studied.

Neuronal cell number is thought to be regulated by *dsx* and *fru* expression. Here, we find that only some *fru*-expressing circadian neuron populations vary in the number of male and female cells detected. The neurons in question are the two transcriptionally related DN3 clusters, which share many defining distinctions from other clock neurons but do not share the same trend in neuron numbers. This leads to the question of how FRU influences neuronal cell numbers. A previous study on *fru* regulation determined that distinct *fru* isoforms affect DN3 cell numbers (Deluca et al., 2024). Recent findings also suggest that the DN3 population contains sleep-promoting neurons (Ma et al., 2025). While that study did not identify specific DN3 subclusters that promote sleep, it suggests that it will be interesting to identify the role of the sexually dimorphic DN3 subclusters shown here in locomotor activity or other behaviors.

GPCRs and neuropeptides are major contributors to neuronal communication. Unlike traditional synaptic communication, GPCR and neuropeptide connections probably do not manifest in connectivity analyses. Nonetheless, these molecules relay messages to other neuronal partners to enable the proper execution of physiological or behavioral outputs. Our lab has previously shown that GPCRs and neuropeptides alone can define adult circadian neuron populations (Ma et al., 2023), and the present study further shows that these connectivity molecules are also sex-enriched within a cell type. The suggestion is that sexually dimorphic GPCRs and neuropeptides contribute to aspects of sexually dimorphic circadian circuits not only during development but also in the fully developed adult nervous system. For example, *Proc* is highly expressed in

female LNds, yet a KO of this neuropeptide decreases locomotor activity in both sexes (data not shown). This suggests that a baseline expression of Proc even in males may promote locomotor activity, whereas the increased *Proc* expression in females may play additional roles in female-specific behaviors such as oviposition, which is known to be regulated by *Proc* expression in other cell types (Belanger & Orchard, 1993).

Further, social enrichment influences mating duration, and GPCR/neuropeptide signaling within circadian lateral neurons is required for this context-dependent mating behavior (Kim et al., 2013). Future studies will likely determine additional roles for these sexually dimorphic GPCRs and neuropeptides in social context-dependent behaviors.

In summary, our work expands upon previous studies by adding the dimension of sex to the transcriptomic profile of *Drosophila* circadian neurons. It includes the identification of sexually dimorphic circadian clusters and genes and provides initial experiments on their connectivity. Understanding more about the regulation of sexually dimorphic gene expression in clock neurons will clarify how sex-specific regulation interacts with environmental factors to influence gene expression and behavioral outputs of the clock network.

Material and Methods

Remapping and clustering published single-cell RNA-seq data set

Single-cell transcriptomic sequencing data was processed using cellranger count version 7 (Zheng et al., 2017). Files were processed individually to obtain FASTQ files and mapped to a newly generated genome containing lncRNAs (dm6). Mapped reads to lncRNAs in each cell were plotted in Fig. S3A. Data integration was done using Seurat V4 (Pereira et al., 2021); a merged RDS object containing the six single-cell experiments (one for each timepoint) was integrated using time as a common variable; this was done via FindIntegrationAnchors and IntegrateData (Pereira et al., 2021). This ensured that the clusters generated were not influenced by cycling gene expression. Cluster identification of this new data set was done by comparing the average gene expression profile of each newly generated cluster to those previously identified (Ma et al., 2021, 2025). Additional validation of cluster identity was done by merging the remapped dataset with the original dataset (Ma et al., 2025), the names of the new clusters coincided with the names of the original clusters.

Fly strains and husbandry for single-cell RNA-seq experiments

Flies were reared on standard cornmeal and agar medium with yeast under 12:12 LD conditions at 25°C. Females used for single-cell experiments were collected as virgins and then paired with males of the same genotype 3 days post-eclosion. Females were co-reared with males for 3 days. A list of flies used in this study can be found in Table S1.

The new single-cell dataset was generated using a genetic multiplexing technique that enables pooled processing of all circadian time points. This approach has previously been used to generate developmental time-series datasets with high temporal resolution

(Kurmangaliyev et al., 2020; Dombrovski et al., 2025). Virgin female flies expressing the Clk856-Gal4 driver were crossed to male flies expressing a nuclear GFP reporter (UAS-His2A-GFP) and carrying one of twelve unique 3rd chromosomes from wild-type strains of the Drosophila Reference Genetic Panel (DGRP, Mackay et al., 2012). Each DGRP chromosome carries a unique set of known single-nucleotide polymorphisms that can be used to separate cells from individual crosses (Kang et al., 2018). F1 flies were collected 1-4 hours after eclosion; sexes were raised separately for 3 days. On day 4, male and female flies with the same DGRP genotype were combined and entrained for 4 days in 12:12 LD. Flies were collected at ZT02, ZT06, ZT10, ZT14, ZT18, and ZT22. Two unique DGRP genotypes were used as biological replicates at each time point, and equal numbers of male and female flies were collected for each genotype. Flies from all time points and DGRP genotypes were combined and processed as a single sample from brain dissections to single-cell dissociation and processing. Two independent samples were generated using this approach.

For the sex-informed data set, virgin female flies expressing Clk856-Gal4 driver and UAS-eGFP were crossed to males expressing a split Gal4 that labels DN3 (R11B03-AD; VT002670-DBD; Ma et al., 2025). F1 progeny were collected 1-4 hours after eclosion. The sexes were raised separately and entrained in 12:12 LD for 3 days. Following entrainment, male and female flies were combined for 2 days and later separated for 3 days in the same LD conditions. Male and female flies were collected separately at ZT06 and ZT18 and put on ice before dissection.

Approximately 200 brains were dissected in ice-cold Schneider's *Drosophila* medium (SM, Gibco #21720001) and then briefly washed with SM and incubated at room

temperature with 0.75ug/ul Collagenase (Sigma-Aldrich #C1639) and 0.04 µg/ul Dispase (Sigma-Aldrich #D4818) for 30 minutes. Brains were washed twice with fresh SM, mechanically triturated to obtain a single cell suspension, and passed through a 40um filter. The volume was adjusted to 3mL for FACS sorting. Nucblue (Invitrogen #R37605) was used to stain for living cells, and GFP was used to isolate the GFP-positive clock neurons via a fluorescence-activated cell sorter (FACS, BDFACS Melody). FACS gates were set using neurons that did not express GFP. 35,000-40,000 GFP-positive cells per replicate were sorted into 500uL of 1XPBS + 0.5% BSA.

Generation of single-cell libraries and raw data processing

Isolated cells were spun down at 1,000rcf for 10 minutes at 4°C using a swing bucket adapter and loaded in the GEM chip from the Chromium Single Cell 3′ Kit (version 3 of 10X Genomics). RNA-seq libraries were prepared using the manufacturer's recommended protocol (CG000315 Rev. B; 10X Genomics). Paired-end sequencing was performed using the Illumina NovaSeq 6000 at 150 cycles. The 10X Cell Ranger package was used to align the sequencing data to the *Drosophila* genome (dm6), including long non-coding RNAs. Reads aligned to annotated exons were quantified using unique molecular identifiers (UMIs) to quantify RNA molecules accurately.

For the new single-cell data set with DGRP chromosomes, single-cell transcriptomes from different timepoints and replicates were demultiplexed based on the unique genotypes of the DGRP chromosomes (Mackay et al., 2012). Demultiplexing was performed using demuxlet (Kang et al., 2018) as described in Dombrovski et al. (Dombrovski et al., 2025)

Data integration and clustering analysis

To retain only high-quality single-cell transcriptomic data, we filtered out cells based on several criteria: 1) the number of detected genes had to be between 500 and 3000, 2) the number of detected UMIs had to be between 1000 and 25000, and 3) the cells with a percentage of mitochondrial RNA greater than 7%.

De novo clustering analysis of the new sex-inferred data set was done using the Seurat package in RStudio (Pereira et al., 2021). High-quality cells from two independent replicates were separated by DGRP line and time using SplitObject, data was normalized, and 2000 variable features were identified using NormalizeData and FindVariableFeatures, respectively. These variable features were used to integrate the datasets using FindIntegrationAnchors and IntegrateData. Clusters were generated using time as a constant to avoid clustering based on time-of-day gene expression. After applying our standard Seurat clustering pipeline (Pereira et al., 2021), we removed only clusters with low *tim* or *Clk* gene expression (for *tim* less than 5 TP10K, for *Clk* less than 1 TP10K), confirmation was done by observing cycling expression of these genes. Cluster identification and naming were done by comparing known marker gene expression from the individual clusters to those established in previous studies (Ma et al., 2021, 2025). Processing and clustering the sex-informed data set was done similarly to the description above. Briefly, the data sets were separated into time points, 2000 variable features were identified, and the common features were used to generate the clusters. Because there is no time course in this experiment, the cycling expression of core clock genes was not used to subset out circadian clusters. Instead, marker gene expression was compared to previously defined clusters (Ma et al., 2025) and confirmed by a correlation matrix between the sex-informed and sex-inferred data sets.

Differential gene expression and Gene Ontology analysis

To identify sex-enriched features within the circadian cell types, we first divided the cells into cell type and sex. With this categorization, we used FindMarkers from the Seurat analysis package to compare the transcriptomic profile between the sexes for each cell type (Pereira et al., 2021). Sex-enriched transcripts were defined by applying the cutoff of an adjusted p-value of < 0.05 and a fold change of 1.7 or greater.

Gene Ontology enrichment analysis was performed using PANGEA (Hu et al., 2023) with genes expressed in all clock neurons as a background gene set. Gene sets used for the analysis included the differentially expressed genes in males or females from the top 4 dimorphic clusters. Log2 normalized counts were used to generate heatmaps illustrating the expression of cell surface molecules, GPCRs, and neuropeptides. Heatmaps were created using the ComplexHeatmap package in RStudio (Gu et al., 2016).

Immunohistochemistry

Flies were fixed by rotating them in 1X PBS with 4% paraformaldehyde (PFA) and 0.5% Triton X-100 for 2.5 hours at room temperature. Following fixation, flies were washed 3X with 1X PBS and 0.5% Triton X-100 (PBST) for 10 minutes each wash at room temperature. Brain dissections were done in 1X PBS solution and blocked with 10X normal goat serum (NGS; Jackson Labs 005-000-121) for 1 hour at room temperature or overnight at 4°C. This was followed by an overnight incubation with primary antibodies against GFP (chicken anti-GFP; Abcam ab13970) and RFP (rat anti-RFP; ProteinTek #5f8) at 4°C. Brains were washed 3X for 15 minutes at room temperature with 0.5% PBST prior to being incubated with secondary antibodies (Alexa Fluor 488 conjugated anti-

chicken, Alexa Fluor 546-conjugated anti-rat diluted at 1:500 in 10X NGS + 0.5% PBST for 2 hours at room temperature. Brains were washed with 0.5% PBST 3X for 15 minutes. Brains were mounted in VectaShield mounting media (Vector Laboratories H-1900-10) and imaged using a Leica Stellaris 8 confocal microscope with a 20X dry or 40X oil objective. Images were processed using FIJI (Schindelin et al., 2015).

Two-photon Functional Calcium Imaging

For *ex vivo*, adult flies were fed with ATR for 3-5 days and dissected during the ZT4-8 period. The fly brains were dissected in hemolymph-like saline (AHL) containing 108mM NaCl, 5mM KCl, 2mM $MgCl_2$, 2mM $CaCl_2$, 4mM $NaHCO_3$, 1mM NaH_2PO_4, 5mM HEPES, 10mM Sucrose, 5mM Trehalose, pH 7.2. The dissected brain was mounted on a special dish containing 1 mL of AHL to prevent movement during imaging. To activate the specific neurons expressing the CsChrimson, we used 630nm red LED illumination (~0.1mW*mm-2) through an optical fiber to illuminate the brain in the dish. For two-photon Ca2+ imaging, we used an Olympus FV1200MPE multiphoton laser scanning microscope equipped with a 25x 0.8NA objective (GCaMP7s excitation @920 nm). Recordings lasted ~120 seconds (two Opto-Stim at 20-35s and 60-75s). Imaging parameters varied slightly between experiments. Images were typically acquired at a resolution of 512x512 pixels and a frame rate of approximately 0.9 Hz. ROIs were analyzed with Fiji. Fluorescence change was calculated using the formula: $\triangle F/F_0 = (F_t-F_0)/F_0\times100\%$ and $\triangle FMax/F_0 = (F_tMax-F_0)/F_0\times100\%$, where F_t is the fluorescence at time n, and F_0 is the fluorescence at time 0.

Generating transgenic flies

Guide RNA transgenic fly lines

Fly lines containing 3X guides under UAS control were generated following previously described protocols (Port & Bullock, 2016; Schlichting et al., 2019). To identify sequences to use as guideRNAs, the CRISPR Optimal Target Finder tool was used (Gratz et al., 2014). Three guides per gene were incorporated into the pCFD6 vector (Addgene #73915) (Port & Bullock, 2016) digested with BbsI-HF restriction enzyme (NEB) using NEBuilder Gibson assembly (NEB E2621S). Correct plasmid sequence was verified by whole plasmid sequencing (Plasmidsaurus) and were sent for embryonic injections into the attP40 or VK00027 sires on the second or third chromosome by Rainbow Transgenic Flies Inc (Camarillo, CA). Primers used for generating UAS-3X-guideRNAs can be found in Table S2.

Ca^{2+} indicator fly line for functional connectivity

The QUAS-jGCaMP7b plasmid was constructed through molecular cloning procedures at Fungene Biotech (http://www.fungene.tech). The coding sequence of jGCaMP7b was PCR-amplified from the 20XUAS-IVS-jGCaMP7b flies (Bloomington Stock Center #79029) using high-fidelity DNA polymerase. The amplified product was subsequently cloned into the pQUAST expression vector (Addgene Plasmid #24349). Finally, the recombinant plasmid was integrated into the VK00005 genomic landing site using site-specific integration techniques to generate stable transgenic lines.

References

Allada, R., White, N. E., So, W. V., Hall, J. C., & Rosbash, M. (1998). A Mutant Drosophila Homolog of Mammalian Clock Disrupts Circadian Rhythms and Transcription of period and timeless. *Cell*, *93*(5), 791–804. https://doi.org/10.1016/S0092-8674(00)81440-3

Belanger, J. H., & Orchard, I. (1993). The Locust Ovipositor Opener Muscle: Proctolinergic Central and Peripheral Neuromodulation in a Centrally Driven Motor System. *Journal of Experimental Biology*, *174*(1), 343–362. https://doi.org/10.1242/jeb.174.1.343

Bell, L. R., Horabin, J. I., Schedl, P., & Cline, T. W. (1991). Positive autoregulation of Sex-lethal by alternative splicing maintains the female determined state in Drosophila. *Cell*, *65*(2), 229–239. https://doi.org/10.1016/0092-8674(91)90157-T

Blanchardon, E., Grima, B., Klarsfeld, A., Chélot, E., Hardin, P. E., Préat, T., & Rouyer, F. (2001). Defining the role of Drosophila lateral neurons in the control of circadian rhythms in motor activity and eclosion by targeted genetic ablation and PERIOD protein overexpression. *European Journal of Neuroscience*, *13*(5), 871–888. https://doi.org/10.1046/j.0953-816x.2000.01450.x

Brovero, S. G., Fortier, J. C., Hu, H., Lovejoy, P. C., Newell, N. R., Palmateer, C. M., Tzeng, R.-Y., Lee, P.-T., Zinn, K., & Arbeitman, M. N. (2021). Investigation of Drosophila fruitless neurons that express Dpr/DIP cell adhesion molecules. *eLife*, *10*, e63101. https://doi.org/10.7554/eLife.63101

Brovkina, M. V., Duffié, R., Burtis, A. E. C., & Clowney, E. J. (2021). Fruitless decommissions regulatory elements to implement cell-type-specific neuronal masculinization. *PLoS Genetics*, *17*(2), e1009338. https://doi.org/10.1371/journal.pgen.1009338

Brown, M. P., Verma, S., Palmer, I., Zuniga, A. G., Mehta, A., Rosensweig, C., Keles, M. F., & Wu, M. N. (2024). A subclass of evening cells promotes the switch from arousal to sleep at dusk. *Current Biology*, *34*(10), 2186-2199.e3. https://doi.org/10.1016/j.cub.2024.04.039

Cachero, S., Ostrovsky, A. D., Yu, J. Y., Dickson, B. J., & Jefferis, G. S. X. E. (2010). Sexual Dimorphism in the Fly Brain. *Current Biology*, *20*(18), 1589–1601. https://doi.org/10.1016/j.cub.2010.07.045

Carrillo, R. A., Özkan, E., Menon, K. P., Nagarkar-Jaiswal, S., Lee, P.-T., Jeon, M., Birnbaum, M. E., Bellen, H. J., Garcia, K. C., & Zinn, K. (2015). Control of Synaptic Connectivity by a Network of *Drosophila* IgSF Cell Surface Proteins. *Cell*, *163*(7), 1770–1782. https://doi.org/10.1016/j.cell.2015.11.022

Certel, S. J., Leung, A., Lin, C.-Y., Perez, P., Chiang, A.-S., & Kravitz, E. A. (2010). Octopamine Neuromodulatory Effects on a Social Behavior Decision-Making Network in Drosophila Males. *PLOS ONE*, *5*(10), e13248. https://doi.org/10.1371/journal.pone.0013248

Chow, C. Y., Wolfner, M. F., & Clark, A. G. (2013). Large Neurological Component to Genetic Differences Underlying Biased Sperm Use in *Drosophila*. *Genetics*, *193*(1), 177–185. https://doi.org/10.1534/genetics.112.146357

Crickmore, M. A., & Vosshall, L. B. (2013). Opposing Dopaminergic and GABAergic Neurons Control the Duration and Persistence of Copulation in Drosophila. *Cell*, *155*(4), 881–893. https://doi.org/10.1016/j.cell.2013.09.055

Deluca, A., Bascom, B., Planas, D. A. K., Kocher, M. A., Torres, M., & Arbeitman, M. N. (2024). *Contribution of neurons that express fruitless and Clock transcription factors to behavioral rhythms and courtship* (p. 2024.06.12.598537). bioRxiv. https://doi.org/10.1101/2024.06.12.598537

Deutsch, D., Pacheco, D., Encarnacion-Rivera, L., Pereira, T., Fathy, R., Clemens, J., Girardin, C., Calhoun, A., Ireland, E., Burke, A., Dorkenwald, S., McKellar, C., Macrina, T., Lu, R., Lee, K., Kemnitz, N., Ih, D., Castro, M., Halageri, A., … Murthy, M. (2020). The neural basis for a persistent internal state in Drosophila females. *eLife*, *9*, e59502. https://doi.org/10.7554/eLife.59502

Dombrovski, M., Zang, Y., Frighetto, G., Vaccari, A., Jang, H., Mirshahidi, P. S., Xie, F., Sanfilippo, P., Hina, B. W., Rehan, A., Hussein, R. H., Mirshahidi, P. S., Lee, C., Morris, A., Frye, M. A., von Reyn, C. R., Kurmangaliyev, Y. Z., Card, G. M., & Zipursky, S. L. (2025). Molecular gradients shape synaptic specificity of a visuomotor transformation. *Nature*, *644*(8076), 453–462. https://doi.org/10.1038/s41586-025-09037-4

Dorkenwald, S., McKellar, C. E., Macrina, T., Kemnitz, N., Lee, K., Lu, R., Wu, J., Popovych, S., Mitchell, E., Nehoran, B., Jia, Z., Bae, J. A., Mu, S., Ih, D., Castro, M., Ogedengbe, O., Halageri, A., Kuehner, K., Sterling, A. R., … Seung, H. S. (2022). FlyWire: Online community for whole-brain connectomics. *Nature Methods*, *19*(1), 119–128. https://doi.org/10.1038/s41592-021-01330-0

Engle, E. C. (2010). Human Genetic Disorders of Axon Guidance. *Cold Spring Harbor Perspectives in Biology*, *2*(3), a001784–a001784. https://doi.org/10.1101/cshperspect.a001784

Epiney, D., Chaya, G. N. M., Dillon, N. R., Lai, S.-L., & Doe, C. Q. (2025). Transcriptional complexity in the insect central complex: Single nuclei RNA-sequencing of adult brain neurons derived from type 2 neuroblasts. *eLife*, *14*. https://doi.org/10.7554/eLife.105896.1

Franke, A., & Baker, B. S. (1999). The *rox1* and *rox2* RNAs Are Essential Components of the Compensasome, which Mediates Dosage Compensation in *Drosophila*. *Molecular Cell*, *4*(1), 117–122. https://doi.org/10.1016/S1097-2765(00)80193-8

Fujii, S., & Amrein, H. (2010). Ventral lateral and DN1 clock neurons mediate distinct properties of male sex drive rhythm in *Drosophila*. *Proceedings of the National Academy of Sciences*, *107*(23), 10590–10595. https://doi.org/10.1073/pnas.0912457107

Fujii, S., Emery, P., & Amrein, H. (2017). SIK3–HDAC4 signaling regulates Drosophila circadian male sex drive rhythm via modulating the DN1 clock neurons. *Proceedings of the National Academy of Sciences of the United States of America*, *114*(32), E6669–E6677. https://doi.org/10.1073/pnas.1620483114

Goldman, T. D., & Arbeitman, M. N. (2007). Genomic and Functional Studies of Drosophila Sex Hierarchy Regulated Gene Expression in Adult Head and Nervous System Tissues. *PLoS Genetics*, *3*(11), e216. https://doi.org/10.1371/journal.pgen.0030216

Gratz, S. J., Ukken, F. P., Rubinstein, C. D., Thiede, G., Donohue, L. K., Cummings, A. M., & O'Connor-Giles, K. M. (2014). Highly specific and efficient CRISPR/Cas9-catalyzed homology-directed repair in Drosophila. *Genetics*, *196*(4), 961–971. https://doi.org/10.1534/genetics.113.160713

Grima, B., Chélot, E., Xia, R., & Rouyer, F. (2004). Morning and evening peaks of activity rely on different clock neurons of the Drosophila brain. *Nature*, *431*(7010), 869–873. https://doi.org/10.1038/nature02935

Gu, Z., Eils, R., & Schlesner, M. (2016). Complex heatmaps reveal patterns and correlations in multidimensional genomic data. *Bioinformatics*, *32*(18), 2847–2849. https://doi.org/10.1093/bioinformatics/btw313

Guo, F., Yu, J., Jung, H. J., Abruzzi, K. C., Luo, W., Griffith, L. C., & Rosbash, M. (2016). Circadian Neuron Feedback Controls the Drosophila Sleep-Activity Profile. *Nature*, *536*(7616), 292–297. https://doi.org/10.1038/nature19097

Hamasaka, Y., Suzuki, T., Hanai, S., & Ishida, N. (2010). Evening circadian oscillator as the primary determinant of rhythmic motivation for Drosophila courtship behavior. *Genes to Cells*, *15*(12), 1240–1248. https://doi.org/10.1111/j.1365-2443.2010.01456.x

Hanafusa, S., Kawaguchi, T., Umezaki, Y., Tomioka, K., & Yoshii, T. (2013). Sexual Interactions Influence the Molecular Oscillations in DN1 Pacemaker Neurons in Drosophila melanogaster. *PLoS ONE*, *8*(12), e84495. https://doi.org/10.1371/journal.pone.0084495

Hauser, F. (2006). Identifying neuropeptide and protein hormone receptors in Drosophila melanogaster by exploiting genomic data. *Briefings in Functional Genomics and Proteomics*, *4*(4), 321–330. https://doi.org/10.1093/bfgp/eli003

Helfrich-Förster, C., Shafer, O. T., Wülbeck, C., Grieshaber, E., Rieger, D., & Taghert, P. (2007). Development and morphology of the clock-gene-expressing lateral neurons of Drosophila melanogaster. *Journal of Comparative Neurology*, *500*(1), 47–70. https://doi.org/10.1002/cne.21146

Helfrich-Förster, C., Yoshii, T., Wülbeck, C., Grieshaber, E., Rieger, D., Bachleitner, W., Cusumano, P., & Rouyer, F. (2007). The Lateral and Dorsal Neurons of *Drosophila melanogaster:* New Insights about Their Morphology and Function. *Cold Spring Harbor Symposia on Quantitative Biology*, *72*(1), 517–525. https://doi.org/10.1101/sqb.2007.72.063

Hewes, R. S., & Taghert, P. H. (2001). Neuropeptides and Neuropeptide Receptors in the *Drosophila melanogaster* Genome. *Genome Research*, *11*(6), 1126–1142. https://doi.org/10.1101/gr.169901

Houl, J. H., Ng, F., Taylor, P., & Hardin, P. E. (2008). CLOCK expression identifies developing circadian oscillator neurons in the brains of Drosophila embryos. *BMC Neuroscience*, *9*(1), 119. https://doi.org/10.1186/1471-2202-9-119

Howlader, G., & Sharma, V. K. (2006). Circadian regulation of egg-laying behavior in fruit flies Drosophila melanogaster. *Journal of Insect Physiology*, *52*(8), 779–785. https://doi.org/10.1016/j.jinsphys.2006.05.001

Hu, Y., Comjean, A., Attrill, H., Antonazzo, G., Thurmond, J., Chen, W., Li, F., Chao, T., Mohr, S. E., Brown, N. H., & Perrimon, N. (2023). PANGEA: A new gene set enrichment tool for *Drosophila* and common research organisms. *Nucleic Acids Research*, *51*(W1), W419–W426. https://doi.org/10.1093/nar/gkad331

Ito, H., Fujitani, K., Usui, K., Shimizu-Nishikawa, K., Tanaka, S., & Yamamoto, D. (1996). Sexual orientation in Drosophila is altered by the satori mutation in the sex-determination gene fruitless that encodes a zinc finger protein with a BTB domain. *Proceedings of the National Academy of Sciences of the United States of America*, *93*(18), 9687–9692. https://doi.org/10.1073/pnas.93.18.9687

Iyer, A. R., Scholz-Carlson, E., Bell, E., Biondi, G., Richhariya, S., & Fernandez, M. P. (2024). *The Circadian Neuropeptide PDF has Sexually Dimorphic Effects on Activity Rhythms* (p. 2024.01.31.578273). bioRxiv. https://doi.org/10.1101/2024.01.31.578273

Jeong, S. (2021). Molecular Mechanisms Underlying Motor Axon Guidance in Drosophila. *Molecules and Cells*, *44*(8), 549–556. https://doi.org/10.14348/molcells.2021.0129

Jung, Y., Kennedy, A., Chiu, H., Mohammad, F., Claridge-Chang, A., & Anderson, D. J. (2020). Neurons that Function within an Integrator to Promote a Persistent Behavioral State in Drosophila. *Neuron*, *105*(2), 322-333.e5. https://doi.org/10.1016/j.neuron.2019.10.028

Kaneko, M., Helfrich-Förster, C., & Hall, J. C. (1997). Spatial and temporal expression of the period and timeless genes in the developing nervous system of Drosophila: Newly identified pacemaker candidates and novel features of clock gene product cycling. *The Journal of Neuroscience: The Official Journal of the Society for Neuroscience*, *17*(17), 6745–6760. https://doi.org/10.1523/JNEUROSCI.17-17-06745.1997

Kang, H. M., Subramaniam, M., Targ, S., Nguyen, M., Maliskova, L., McCarthy, E., Wan, E., Wong, S., Byrnes, L., Lanata, C. M., Gate, R. E., Mostafavi, S., Marson, A., Zaitlen, N., Criswell, L. A., & Ye, C. J. (2018). Multiplexed droplet single-cell RNA-sequencing using natural genetic variation. *Nature Biotechnology*, *36*(1), 89–94. https://doi.org/10.1038/nbt.4042

Kim, W. J., Jan, L. Y., & Jan, Y. N. (2012). Contribution of visual and circadian neural circuits to memory for prolonged mating induced by rivals. *Nature Neuroscience*, *15*(6), 876–883. https://doi.org/10.1038/nn.3104

Kim, W. J., Jan, L. Y., & Jan, Y. N. (2013). A PDF/NPF Neuropeptide Signaling Circuitry of Male Drosophila melanogaster Controls Rival-Induced Prolonged Mating. *Neuron*, *80*(5), 1190–1205. https://doi.org/10.1016/j.neuron.2013.09.034

Kurmangaliyev, Y. Z., Yoo, J., Valdes-Aleman, J., Sanfilippo, P., & Zipursky, S. L. (2020). Transcriptional Programs of Circuit Assembly in the Drosophila Visual System. *Neuron*, *108*(6), 1045-1057.e6. https://doi.org/10.1016/j.neuron.2020.10.006

Le, J. Q., Ma, D., Dai, X., & Rosbash, M. (2024). Light and dopamine impact two circadian neurons to promote morning wakefulness. *Current Biology: CB*, *34*(17), 3941-3954.e4. https://doi.org/10.1016/j.cub.2024.07.056

Lee, G., Bahn, J. H., & Park, J. H. (2006). Sex- and clock-controlled expression of the neuropeptide F gene in Drosophila. *Proceedings of the National Academy of Sciences*, *103*(33), 12580–12585. https://doi.org/10.1073/pnas.0601171103

Lee, G., Foss, M., Goodwin, S. F., Carlo, T., Taylor, B. J., & Hall, J. C. (2000). Spatial, temporal, and sexually dimorphic expression patterns of the fruitless gene in the Drosophila central nervous system. *Journal of Neurobiology*, *43*(4), 404–426. https://doi.org/10.1002/1097-4695(20000615)43:4<404::AID-NEU8>3.0.CO;2-D

Ma, B., Wang, R., Liu, Y., Deng, B., Wang, T., Wu, F., & Zhou, C. (2022). Serotonin Signaling Modulates Sexual Receptivity of Virgin Female Drosophila. *Neuroscience Bulletin*, *38*(11), 1277–1291. https://doi.org/10.1007/s12264-022-00908-8

Ma, D., Herndon, N., Le, J. Q., Abruzzi, K. C., Zinn, K., & Rosbash, M. (2023). Neural connectivity molecules best identify the heterogeneous clock and dopaminergic cell types in the Drosophila adult brain. *Science Advances*, *9*(8), eade8500. https://doi.org/10.1126/sciadv.ade8500

Ma, D., Le, J. Q., Dai, X., Díaz, M. M., Abruzzi, K. C., & Rosbash, M. (2025). Transcriptomic DN3 clock neuron subtypes regulate Drosophila sleep. *Science Advances*, *11*(1), eadr4580. https://doi.org/10.1126/sciadv.adr4580

Ma, D., Przybylski, D., Abruzzi, K. C., Schlichting, M., Li, Q., Long, X., & Rosbash, M. (2021). A transcriptomic taxonomy of Drosophila circadian neurons around the clock. *eLife*, *10*, e63056. https://doi.org/10.7554/eLife.63056

Mackay, T. F. C., Richards, S., Stone, E. A., Barbadilla, A., Ayroles, J. F., Zhu, D., Casillas, S., Han, Y., Magwire, M. M., Cridland, J. M., Richardson, M. F., Anholt, R. R. H., Barrón, M., Bess, C., Blankenburg, K. P., Carbone, M. A., Castellano, D., Chaboub, L., Duncan, L., … Gibbs, R. A. (2012). The Drosophila melanogaster Genetic Reference Panel. *Nature*, *482*(7384), 173–178. https://doi.org/10.1038/nature10811

Manjunatha, T., Dass, S. H., & Sharma, V. K. (2008). Egg-laying rhythm in Drosophila melanogaster. *Journal of Genetics*, *87*(5), 495–504. https://doi.org/10.1007/s12041-008-0072-9

Meller, V. H., & Rattner, B. P. (2002). The roX genes encode redundant male-specific lethal transcripts required for targeting of the MSL complex. *The EMBO Journal*, *21*(5), 1084–1091. https://doi.org/10.1093/emboj/21.5.1084

Mellert, D. J., Knapp, J.-M., Manoli, D. S., Meissner, G. W., & Baker, B. S. (2010). Midline crossing by gustatory receptor neuron axons is regulated by fruitless, doublesex and the Roundabout receptors. *Development*, *137*(2), 323–332. https://doi.org/10.1242/dev.045047

Moschall, R., Rass, M., Rossbach, O., Lehmann, G., Kullmann, L., Eichner, N., Strauss, D., Meister, G., Schneuwly, S., Krahn, M. P., & Medenbach, J. (2019). Drosophila Sister-of-Sex-lethal reinforces a male-specific gene expression pattern by controlling Sex-lethal alternative splicing. *Nucleic Acids Research*, *47*(5), 2276–2288. https://doi.org/10.1093/nar/gky1284

Myers, E. M., Yu, J., & Sehgal, A. (2003). Circadian Control of Eclosion: Interaction between a Central and Peripheral Clock in Drosophila melanogaster. *Current Biology*, *13*(6), 526–533. https://doi.org/10.1016/S0960-9822(03)00167-2

Nässel, D. R., & Zandawala, M. (2020). Hormonal axes in Drosophila: Regulation of hormone release and multiplicity of actions. *Cell and Tissue Research*, *382*(2), 233–266. https://doi.org/10.1007/s00441-020-03264-z

Palmateer, C. M., Artikis, C., Brovero, S. G., Friedman, B., Gresham, A., & Arbeitman, M. N. (2023). Single-cell transcriptome profiles of Drosophila fruitless-expressing neurons from both sexes. *eLife*, *12*, e78511. https://doi.org/10.7554/eLife.78511

Pereira, W. J., Almeida, F. M., Conde, D., Balmant, K. M., Triozzi, P. M., Schmidt, H. W., Dervinis, C., Pappas, G. J., & Kirst, M. (2021). Asc-Seurat: Analytical single-cell

Seurat-based web application. *BMC Bioinformatics*, *22*(1), 556. https://doi.org/10.1186/s12859-021-04472-2
Picot, M., Klarsfeld, A., Chélot, E., Malpel, S., & Rouyer, F. (2009). A Role for Blind DN2 Clock Neurons in Temperature Entrainment of the Drosophila Larval Brain. *The Journal of Neuroscience*, *29*(26), 8312–8320. https://doi.org/10.1523/JNEUROSCI.0279-08.2009
Poe, A. R., Zhu, L., Szuperak, M., McClanahan, P. D., Anafi, R. C., Scholl, B., Thum, A. S., Cavanaugh, D. J., & Kayser, M. S. (2023). Developmental emergence of sleep rhythms enables long-term memory in Drosophila. *Science Advances*, *9*(36), eadh2301. https://doi.org/10.1126/sciadv.adh2301
Port, F., & Bullock, S. L. (2016). Augmenting CRISPR applications in Drosophila with tRNA-flanked sgRNAs. *Nature Methods*, *13*(10), 852–854. https://doi.org/10.1038/nmeth.3972
Reinhard, N., Fukuda, A., Manoli, G., Derksen, E., Saito, A., Möller, G., Sekiguchi, M., Rieger, D., Helfrich-Förster, C., Yoshii, T., & Zandawala, M. (2024). Synaptic connectome of the Drosophila circadian clock. *Nature Communications*, *15*(1), 10392. https://doi.org/10.1038/s41467-024-54694-0
Rideout, E. J., Dornan, A. J., Neville, M. C., Eadie, S., & Goodwin, S. F. (2010). Control of sexual differentiation and behavior by the doublesex gene in Drosophila melanogaster. *Nature Neuroscience*, *13*(4), 458–466. https://doi.org/10.1038/nn.2515
Riva, S., Ceriani, M. F., Risau-Gusman, S., & Franco, D. L. (2024). *Circadian control of a sex-specific behaviour in Drosophila* (p. 2024.03.27.586991). bioRxiv. https://doi.org/10.1101/2024.03.27.586991
Sakai, T., & Ishida, N. (2001). Circadian rhythms of female mating activity governed by clock genes in Drosophila. *Proceedings of the National Academy of Sciences of the United States of America*, *98*(16), 9221–9225. https://doi.org/10.1073/pnas.151443298
Schindelin, J., Rueden, C. T., Hiner, M. C., & Eliceiri, K. W. (2015). The ImageJ ecosystem: An open platform for biomedical image analysis. *Molecular Reproduction and Development*, *82*(7–8), 518–529. https://doi.org/10.1002/mrd.22489
Schlichting, M., Díaz, M. M., Xin, J., & Rosbash, M. (2019). Neuron-specific knockouts indicate the importance of network communication to Drosophila rhythmicity. *eLife*, *8*, e48301. https://doi.org/10.7554/eLife.48301
Schlichting, M., Richhariya, S., Herndon, N., Ma, D., Xin, J., Lenh, W., Abruzzi, K., & Rosbash, M. (2022). Dopamine and GPCR-mediated modulation of DN1 clock neurons gates the circadian timing of sleep. *Proceedings of the National Academy of Sciences*, *119*(34), e2206066119. https://doi.org/10.1073/pnas.2206066119
Schubert, F. K., Hagedorn, N., Yoshii, T., Helfrich-Förster, C., & Rieger, D. (2018). Neuroanatomical details of the lateral neurons of *Drosophila melanogaster* support their functional role in the circadian system. *Journal of Comparative Neurology*, *526*(7), 1209–1231. https://doi.org/10.1002/cne.24406
Shafer, O. T., Gutierrez, G. J., Li, K., Mildenhall, A., Spira, D., Marty, J., Lazar, A. A., & Fernandez, M. de la P. (2022). Connectomic analysis of the Drosophila lateral

neuron clock cells reveals the synaptic basis of functional pacemaker classes. *eLife*, *11*, e79139. https://doi.org/10.7554/eLife.79139

Sheeba, V., Kaneko, M., Sharma, V. K., & Holmes, T. C. (2008). The Drosophila Circadian Pacemaker Circuit: Pas de Deux or Tarantella? *Critical Reviews in Biochemistry and Molecular Biology*, *43*(1), 37–61. https://doi.org/10.1080/10409230701829128

Stoleru, D., Peng, Y., Agosto, J., & Rosbash, M. (2004). Coupled oscillators control morning and evening locomotor behaviour of Drosophila. *Nature*, *431*(7010), 862–868. https://doi.org/10.1038/nature02926

Sun, L., Jiang, R. han, Ye, W. jing, Rosbash, M., & Guo, F. (2022a). Recurrent circadian circuitry regulates central brain activity to maintain sleep. *Neuron*, *110*(13), 2139-2154.e5. https://doi.org/10.1016/j.neuron.2022.04.010

Sun, L., Jiang, R. H., Ye, W. J., Rosbash, M., & Guo, F. (2022b). Recurrent circadian circuitry regulates central brain activity to maintain sleep. *Neuron*, *110*(13), 2139-2154.e5. https://doi.org/10.1016/j.neuron.2022.04.010

Talay, M., Richman, E. B., Snell, N. J., Hartmann, G. G., Fisher, J. D., Sorkaç, A., Santoyo, J. F., Chou-Freed, C., Nair, N., Johnson, M., Szymanski, J. R., & Barnea, G. (2017). Transsynaptic Mapping of Second-Order Taste Neurons in Flies by trans-Tango. *Neuron*, *96*(4), 783-795.e4. https://doi.org/10.1016/j.neuron.2017.10.011

Villella, A., & Hall, J. C. (1996). Courtship Anomalies Caused by doublesex Mutations in Drosophila melanogaster. *Genetics*, *143*(1), 331–344. https://doi.org/10.1093/genetics/143.1.331

Wang, K., Wang, F., Forknall, N., Yang, T., Patrick, C., Parekh, R., & Dickson, B. J. (2021). Neural circuit mechanisms of sexual receptivity in Drosophila females. *Nature*, *589*(7843), 577–581. https://doi.org/10.1038/s41586-020-2972-7

Yoshii, T., Hermann, C., & Helfrich-Förster, C. (2010). Cryptochrome-Positive and -Negative Clock Neurons in Drosophila Entrain Differentially to Light and Temperature. *Journal of Biological Rhythms*, *25*(6), 387–398. https://doi.org/10.1177/0748730410381962

Yu, J. Y., Kanai, M. I., Demir, E., Jefferis, G. S. X. E., & Dickson, B. J. (2010). Cellular Organization of the Neural Circuit that Drives Drosophila Courtship Behavior. *Current Biology*, *20*(18), 1602–1614. https://doi.org/10.1016/j.cub.2010.08.025

Zhang, C., Daubnerova, I., Jang, Y.-H., Kondo, S., Žitňan, D., & Kim, Y.-J. (2021). The neuropeptide allatostatin C from clock-associated DN1p neurons generates the circadian rhythm for oogenesis. *Proceedings of the National Academy of Sciences of the United States of America*, *118*(4), e2016878118. https://doi.org/10.1073/pnas.2016878118

Zhang, S. X., Rogulja, D., & Crickmore, M. A. (2016). Dopaminergic Circuitry Underlying Mating Drive. *Neuron*, *91*(1), 168–181. https://doi.org/10.1016/j.neuron.2016.05.020

Zheng, G. X. Y., Terry, J. M., Belgrader, P., Ryvkin, P., Bent, Z. W., Wilson, R., Ziraldo, S. B., Wheeler, T. D., McDermott, G. P., Zhu, J., Gregory, M. T., Shuga, J., Montesclaros, L., Underwood, J. G., Masquelier, D. A., Nishimura, S. Y., Schnall-Levin, M., Wyatt, P. W., Hindson, C. M., … Bielas, J. H. (2017). Massively parallel

digital transcriptional profiling of single cells. *Nature Communications*, *8*(1), 14049. https://doi.org/10.1038/ncomms14049

Zhou, C., Franconville, R., Vaughan, A. G., Robinett, C. C., Jayaraman, V., & Baker, B. S. (2015). Central neural circuitry mediating courtship song perception in male Drosophila. *eLife*, *4*, e08477. https://doi.org/10.7554/eLife.08477

Zhou, C., Pan, Y., Robinett, C. C., Meissner, G. W., & Baker, B. S. (2014). Central Brain Neurons Expressing doublesex Regulate Female Receptivity in Drosophila. *Neuron*, *83*(1), 149–163. https://doi.org/10.1016/j.neuron.2014.05.038

Zhou, C., Rao, Y., & Rao, Y. (2008). A subset of octopaminergic neurons are important for Drosophila aggression. *Nature Neuroscience*, *11*(9), 1059–1067. https://doi.org/10.1038/nn.2164

Zinn, K., & Özkan, E. (2017). Neural immunoglobulin superfamily interaction networks. *Current Opinion in Neurobiology*, *45*, 99–105. https://doi.org/10.1016/j.conb.2017.05.010

Figure 1. Identification of sexually dimorphic circadian transcriptomic clusters

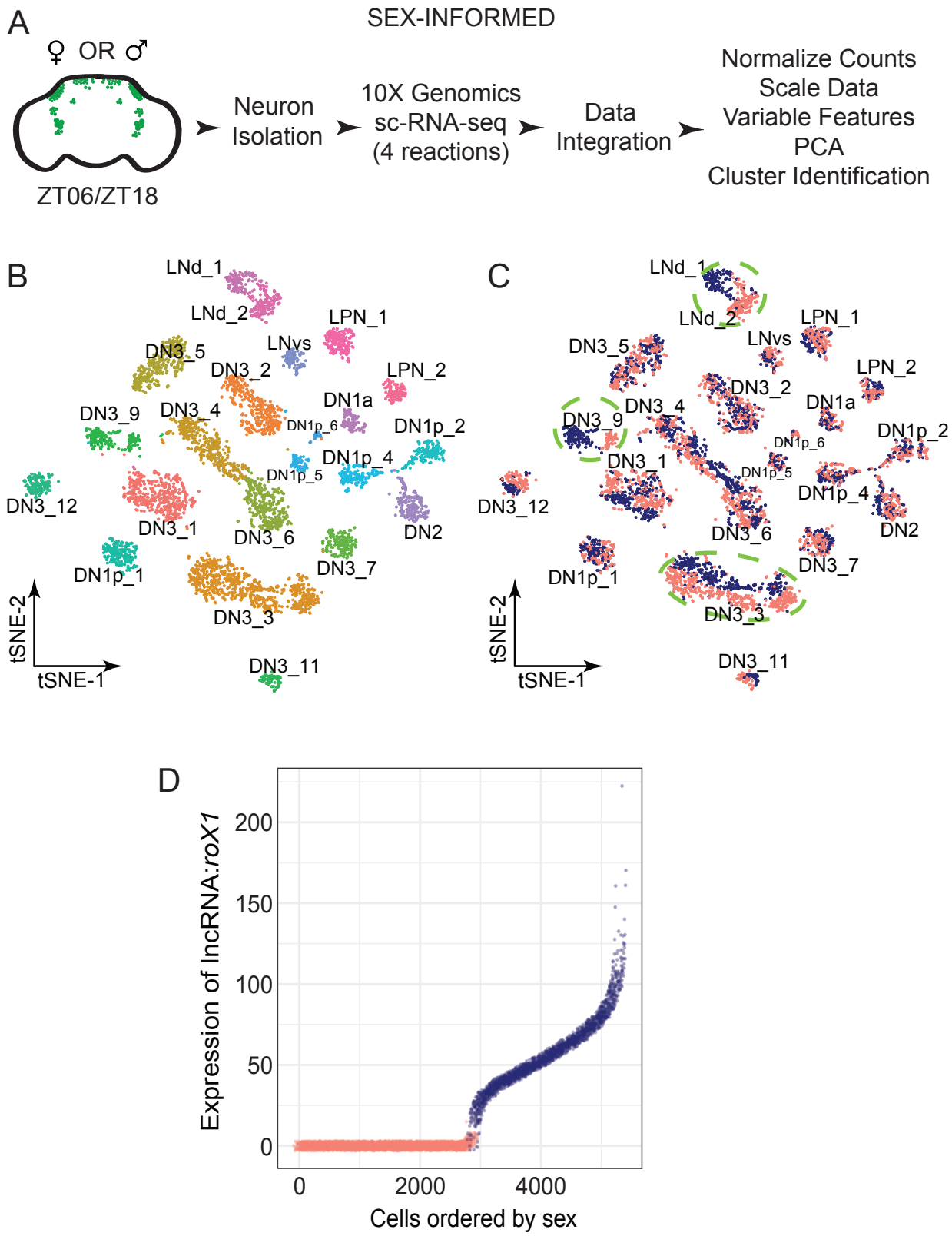

Figure 1. Identification of sexually dimorphic circadian transcriptomic clusters (continued)

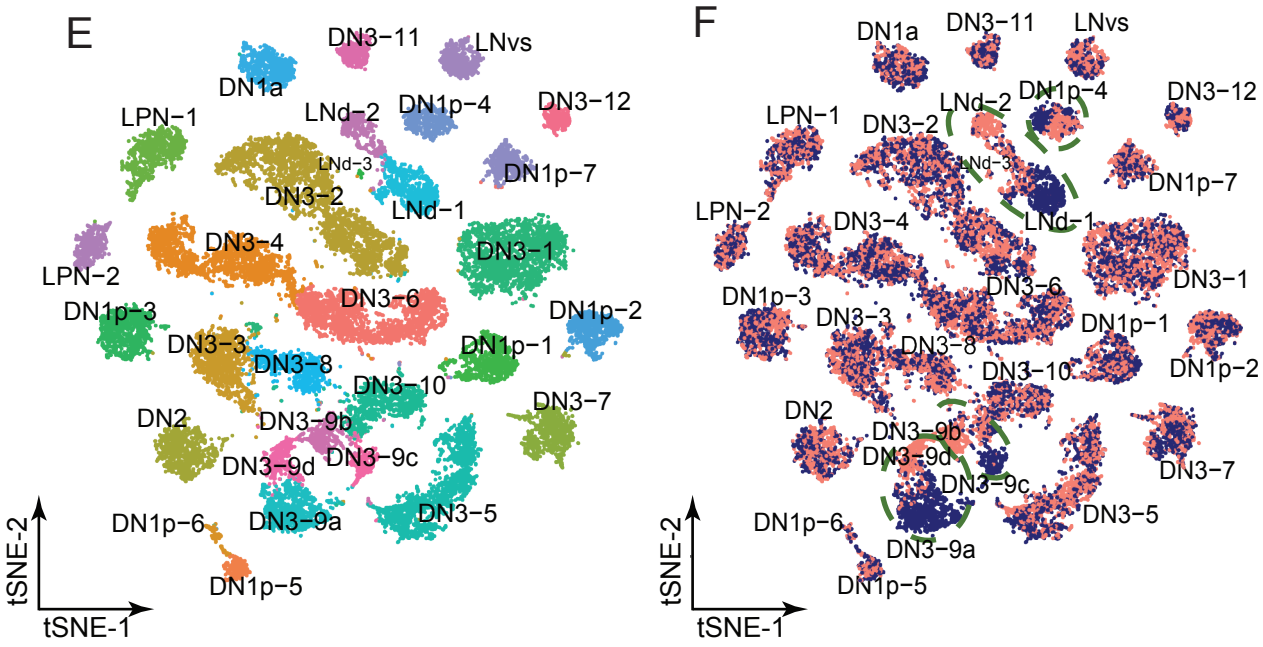

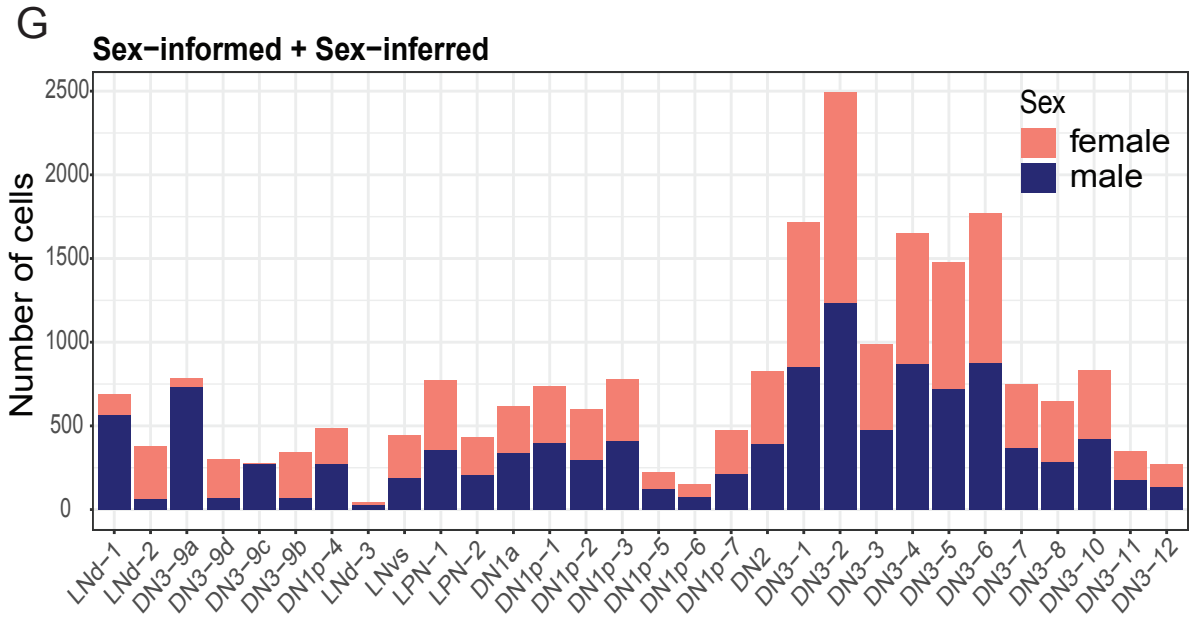

Figure 2. Sexually dimorphic gene expression of circadian neurons is cell-type-specific

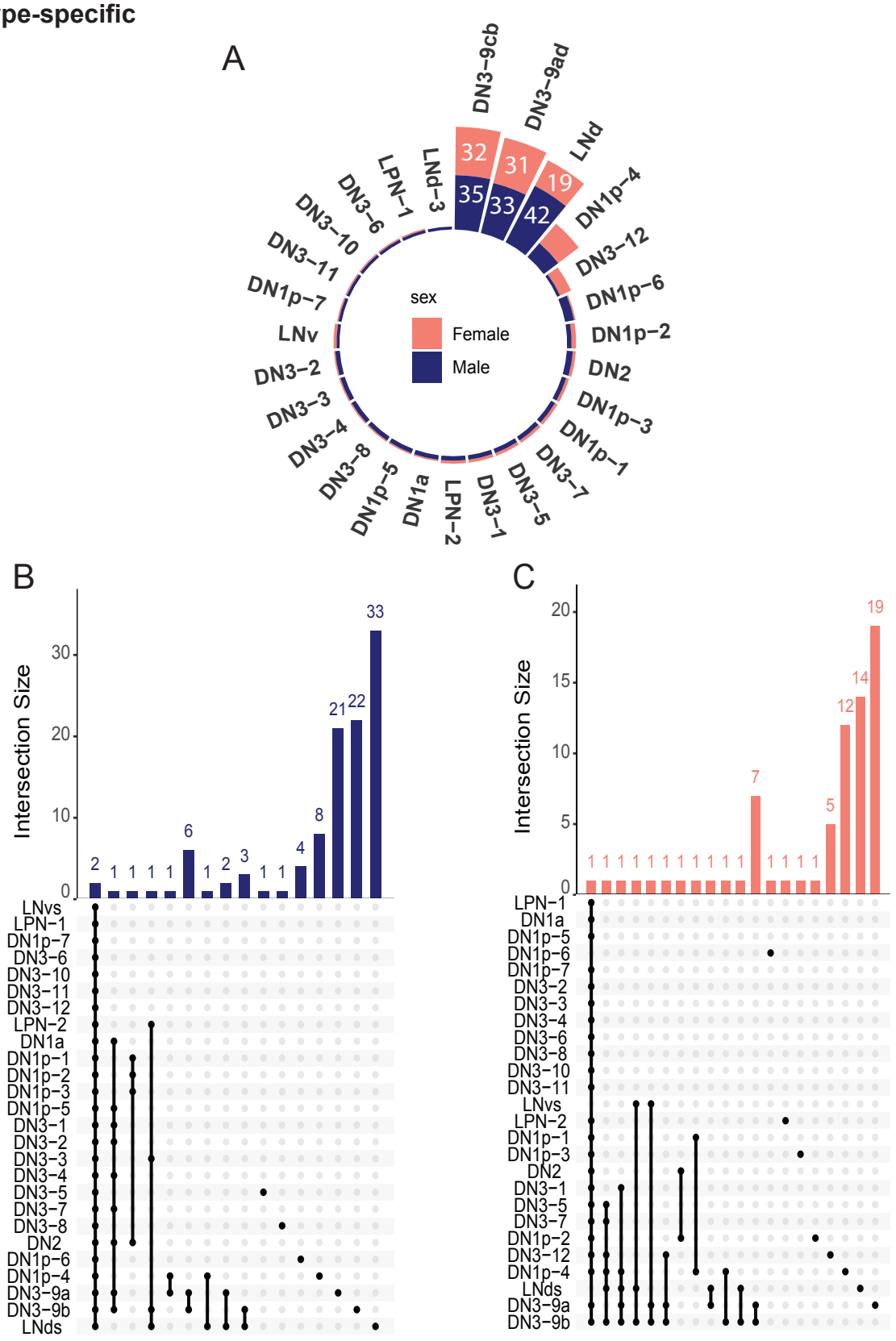

Figure 3. Sex-specific connectivity molecules are expressed in the sexually dimorphic circadian neurons

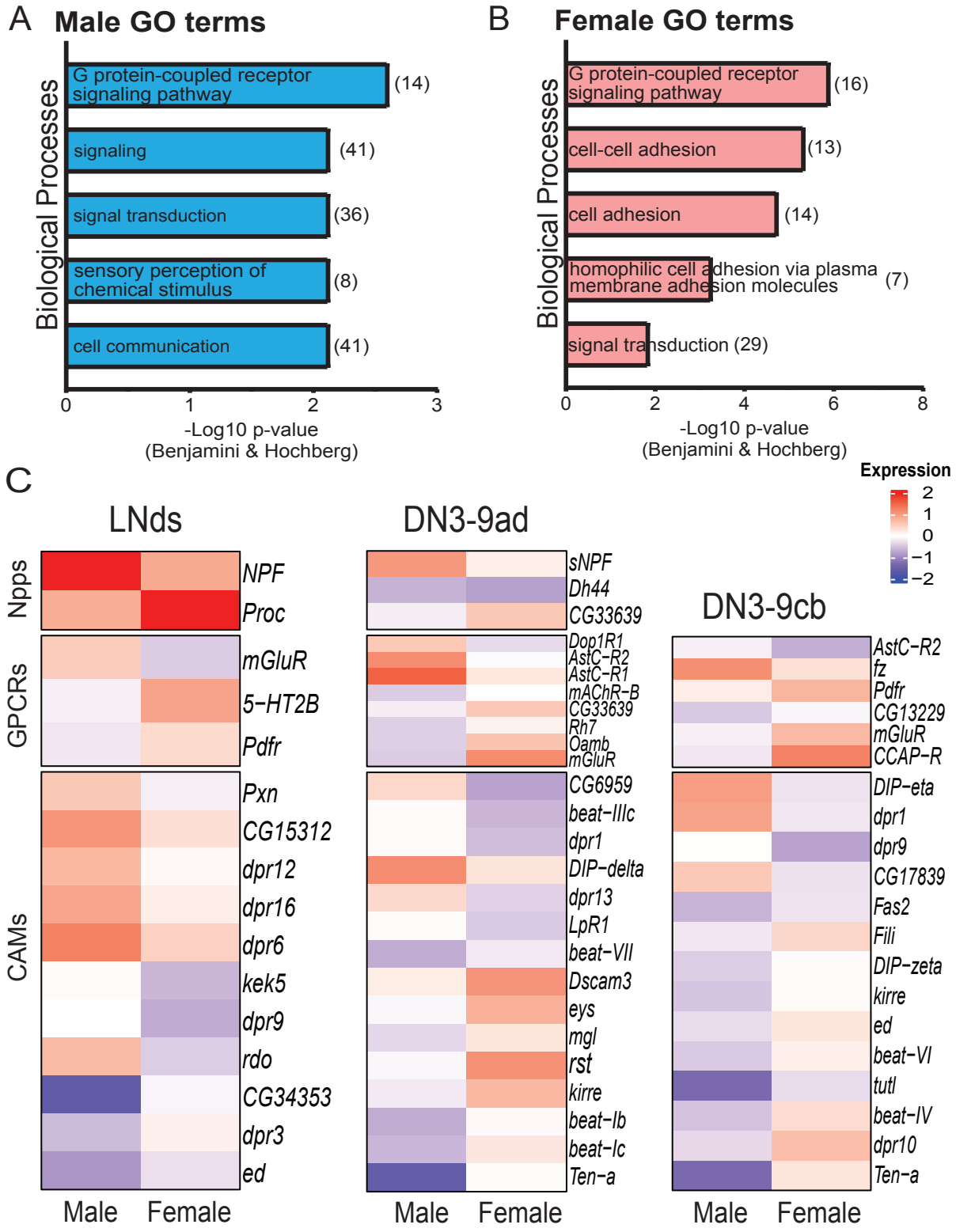

Figure 3. Sex-specific connectivity molecules are expressed in the sexually dimorphic circadian neurons (continued)

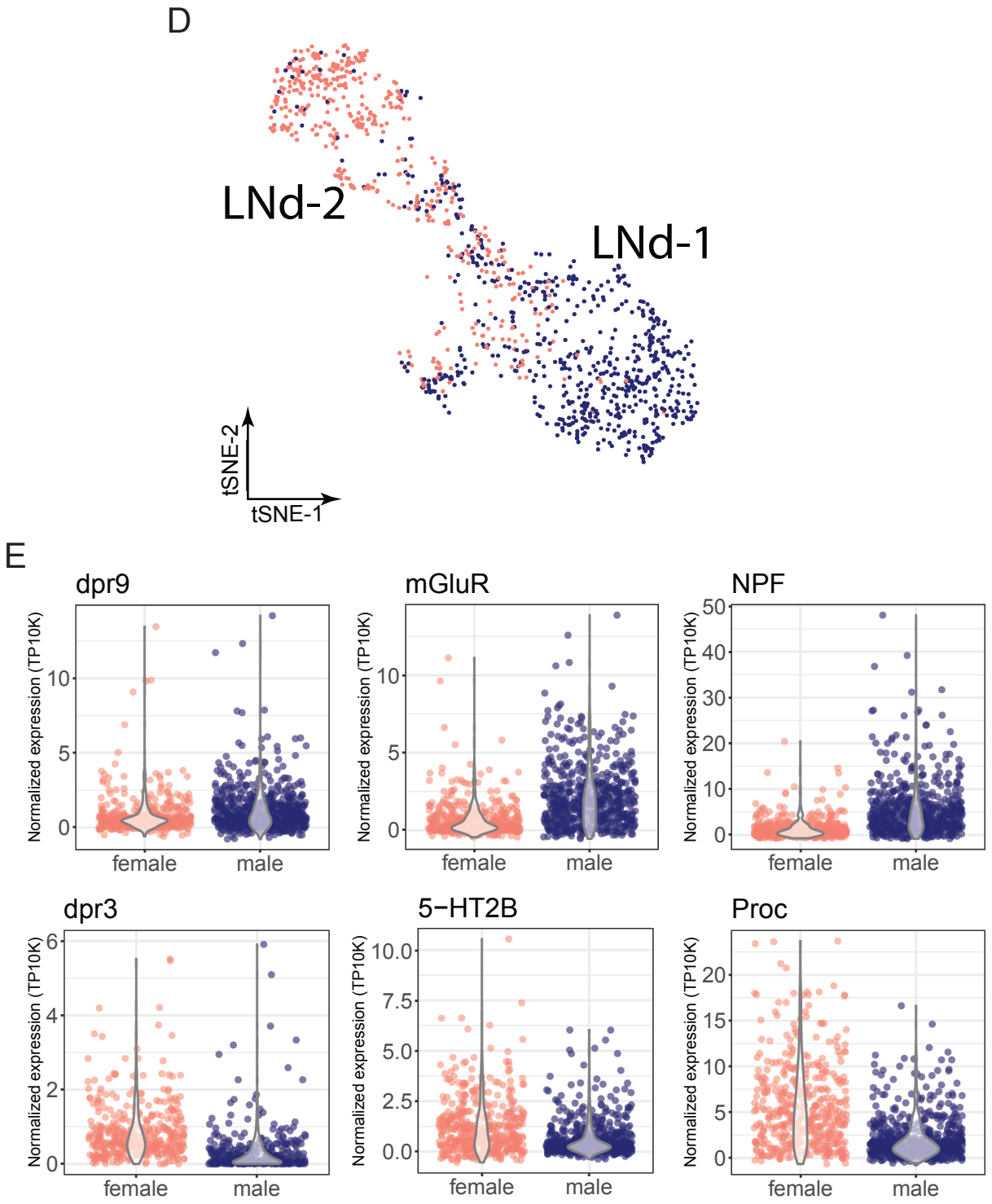

Figure 4. Circadian LNds are upstream of *dsx*-expressing pC1 and pCd neurons

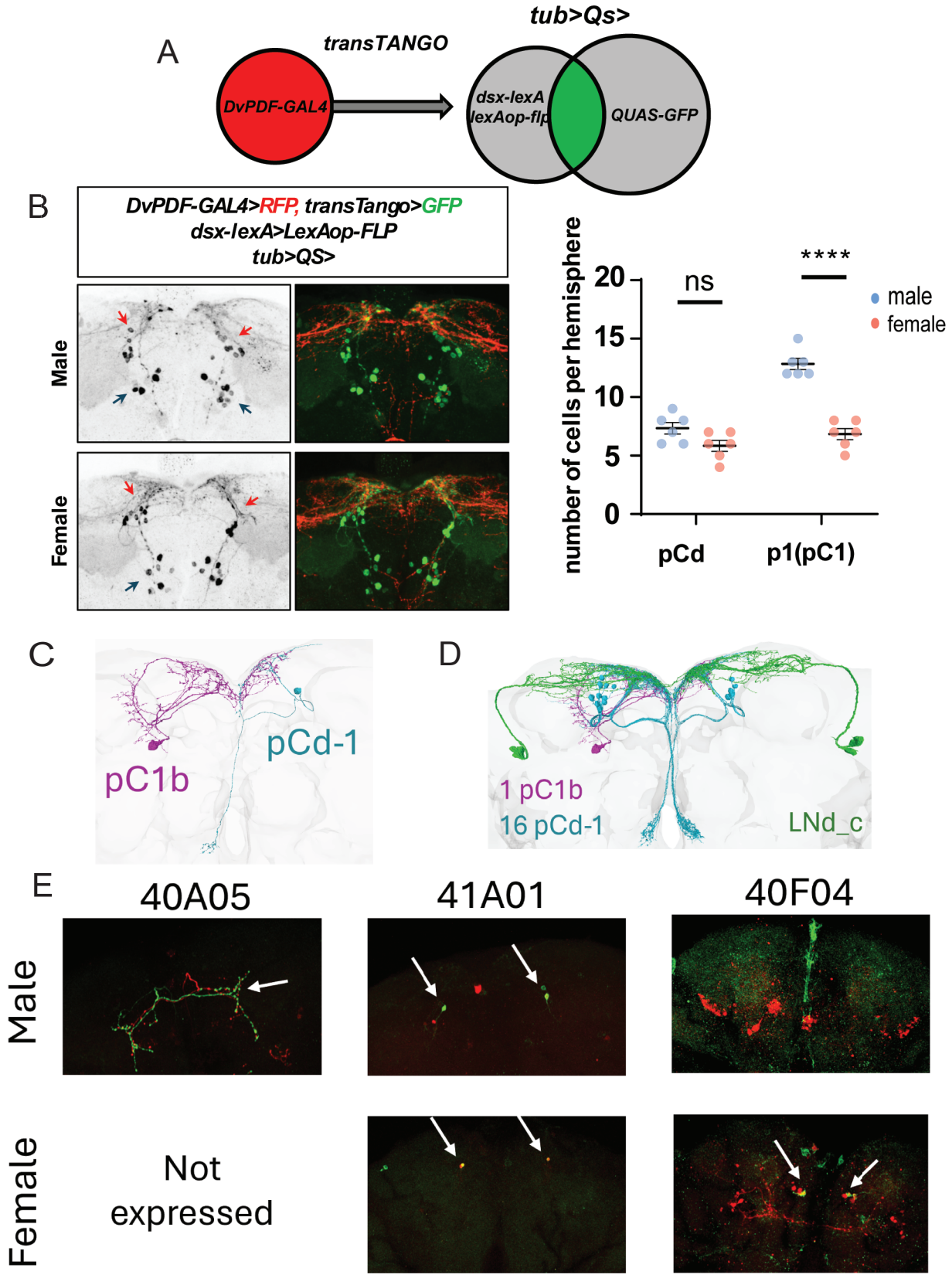

Figure 5. Sex-enriched CAMs in the LNds mediate synaptic connection to *dsx*-positive neurons

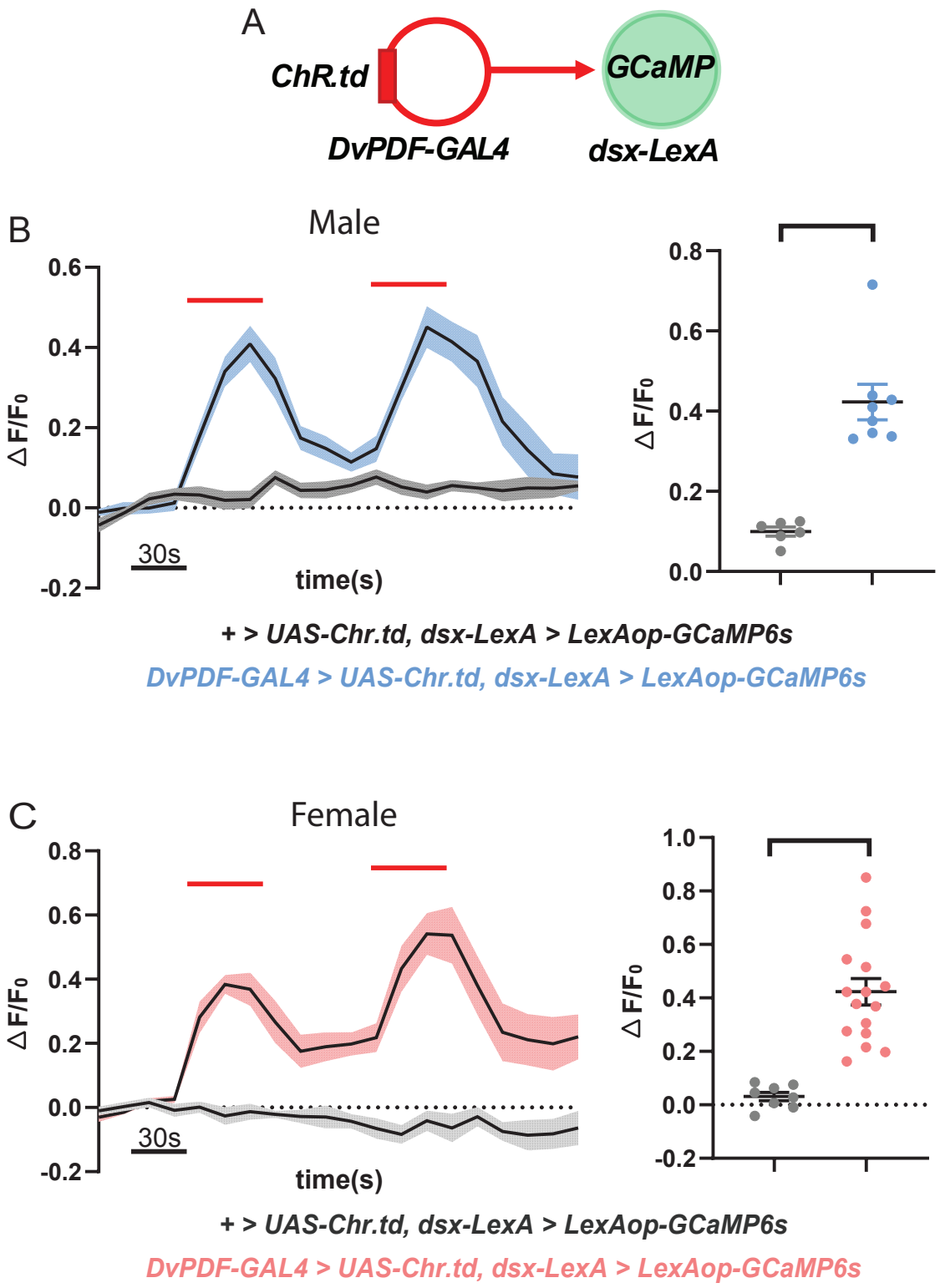

Figure 5. Sex-enriched CAMs in the LNds mediate synaptic connection to *dsx*-positive neurons (continued)

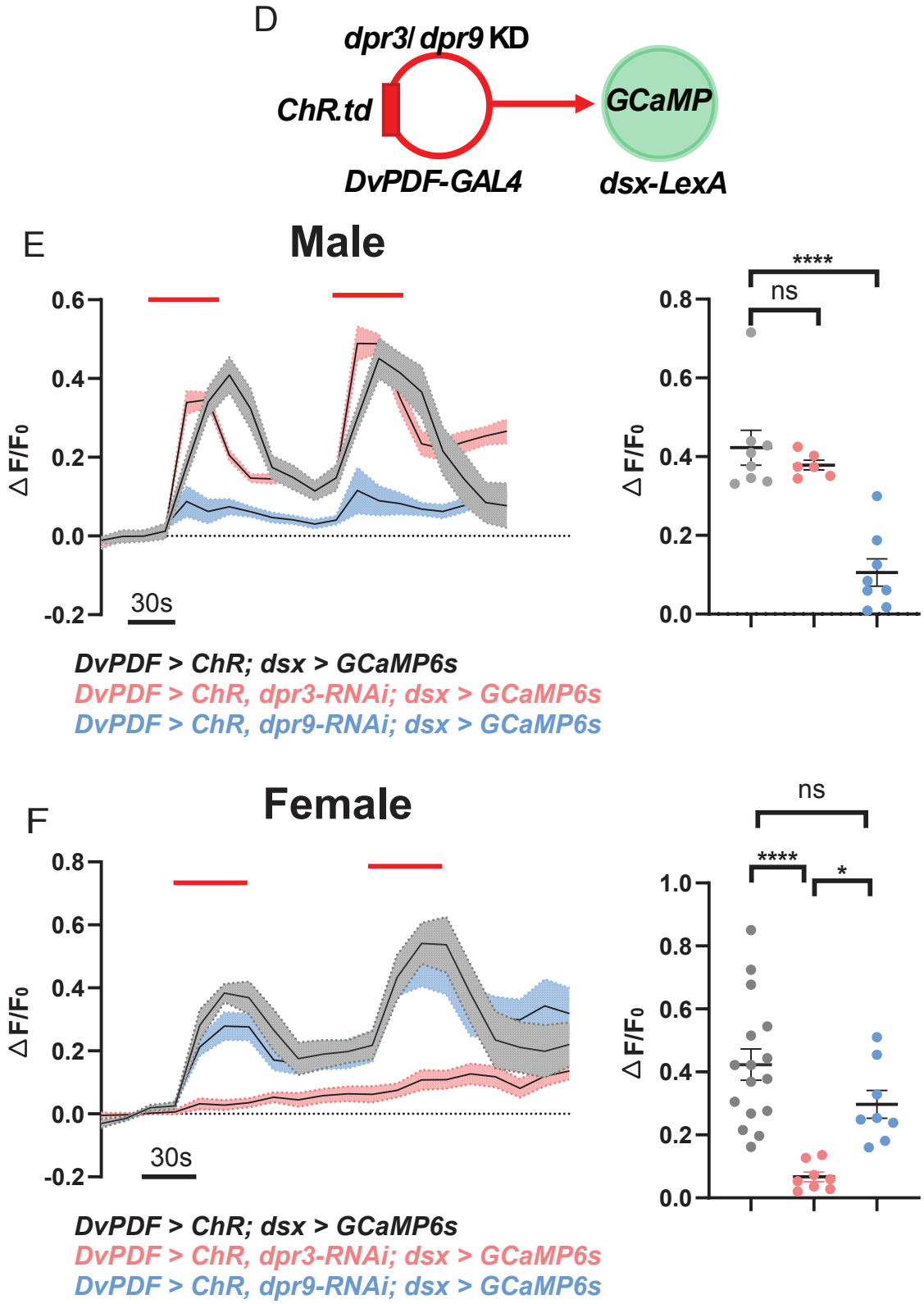

Figure Legends

Figure 1. Identification of sexually dimorphic circadian transcriptomic clusters.

(A) Schematics of experimental design for generating and processing single cells RNA sequencing of male and female circadian neurons. Male and female flies with GFP labeled circadian neurons were collected at two time points (ZT06 and ZT18). Male and female samples were collected and handled separately. GFP-positive circadian neurons were isolated using FACS, and single-cell RNA sequencing libraries were generated using single-cell 3' RNA seq (10X Genomics). Genome alignment and data processing was carried out using CellRanger and Seurat packages, respectively. (B) Dimensional reduction plot of the de novo clustering identities from the newly generated sex-informed circadian single cell data set. Each color represents a distinct circadian cell type. (C) Dimensional reduction plot of the circadian clusters grouped by sex. Green dashed lines show sex-biased circadian transcriptomic clusters. (D) Normalized expression plot of *lncRNA:roX1*. X axis shows high confidence circadian neurons; pink dots show the female-derived cells and blue dots show the male derived cells. Y axis shows *lncRNA:roX1* normalized expression from the sex-informed dataset. (E) Dimensional reduction plot of the integrated sex-informed and sex-inferred datasets. Each color represents a distinct circadian cell type. (F) Dimensional reduction plot of the integrated sex-informed and sex-inferred datasets grouped by inferred sex based on ROC determined cutoffs for optimal sex-calling. Green dashed lines show sex-biased circadian transcriptomic clusters. (G) Number of male and female cells in integrated data set plotted by cell type. Pink bars show number of female cells; blue bars show number of male cells per cluster. Brackets indicate the sex-biased clusters.

Figure 2. Sexually dimorphic gene expression of circadian neurons is cell-type-specific.

(A) Bar plot showing number of differentially expressed genes (DEGs) between males and females for each individual cluster. Pink bars show number of female DEGs, blue bars show number of male DEGs. (B) Gene intersection plot of all genes upregulated in male circadian neurons in each cluster. Horizontal blue lines show to the gene set size, which represents the total number of male upregulated genes in each cluster. Black dots and vertical black lines show an intersection of common genes between the clusters. The vertical blue line shows the number of common genes for each identified intersection. (C) Gene intersection plot of all female upregulated genes in each cluster. Horizontal pink lines show the gene set size, which represents the total number of female upregulated genes in each cluster. Black dots and vertical black lines show an intersection of common genes between the clusters. Vertical pink line shows the number of common genes for each identified intersection.

Figure 3. Sex-specific connectivity molecules are expressed in the sexually dimorphic circadian neurons.

(A-B) Gene ontology analysis of (A) male and (B) female enriched genes in the sexually dimorphic circadian cell types. X axis shows –LOG10 p-value of each enriched gene group identified. Numbers in parenthesis show the number of genes identified in the dataset that form part of the gene ontology term (Benjamini & Hochberg p-value less than 0.01). (C) Heatmap visualizing gene expression (normalized Log2 scale) of sexually dimorphic gene groups in the LNds (left), DN3-9a/d (middle) and DN3-9c/b (right) clusters. (D) Dimensional reduction plot of the male (blue) and female (pink) cell distribution of the sexually dimorphic LNd cluster. (E) Normalized expression of neural connectivity molecules enriched in either male (top) or female (bottom) LNds. From left to right: CAMs, GPCRs and neuropeptides.

Figure 4. Circadian LNds are upstream of dsx-expressing pC1 and pCd neurons.

(A) Schematic representation of restricted transTANGO approach to identify potential synaptic connections between two neuronal cell types. Gal4-labeled neurons drive the expression of transTANGO presynaptic ligand. LexA-labeled neurons drive the expression of a LexAop-FLP. This allows only the LexA-expressing neurons to flip out a STOP codon and promote the expression of the TF QS, which, in turn, promotes the expression of GFP (QUAS-GFP) in downstream neuronal subsets of interest. (B) Restricted transTANGO of male and female brains between *DvPDF-Gal4* and *dsx-LexA*. RFP is expressed in all *dsx-LexA*-expressing neurons, GFP is expressed in *dsx-LexA*-labeled neurons, which are post-synaptically connected to *DvPDF*-expressing neurons. The right panel shows the number of detected dsx-expressing neurons downstream of *DvPDF*-expressing neurons. pC1 and pCd neuronal subtypes were identified by anatomical location and projection patterns. (C) Representative projection patterns of pC1 (left) and pCd (right) neuronal subtype from FlyWire EM connectome. (D) Predicted dsx-expressing neurons downstream of circadian E3 LNd subtype from FlyWire EM connectome. Neurons in green show E3 LNds, neurons in magenta and blue show predicted pC1 and pCd neurons, respectively. (E) Restricted transTANGO of male and female brains between *DvPDF-Gal4* and three sparse LexA drivers labeling (left) pC1-40A05, (middle) pCd-41A01, and (right) pC1 and pC2-40F04 dsx-expressing neuronal subsets. 40F04 male samples did not show GFP labeling. Female brains from 40F04 shows pC1 neurons labeled in green. GFP is expressed in dsx- LexA-labeled neurons which are post-synaptically connected to DvPDF-expressing neurons. White arrows show GFP-positive dsx-expressing neuronal populations.

Figure 5. Sex-enriched CAMs in the LNds mediate synaptic connection to dsx-positive neurons.

(A,D) Schematic representation of live imaging dsx-expressing neurons containing a Ca2+ indicator upon optogenetic activation of *DvPDF*-expressing neurons. (B-C) Male (B) and female (C) Ca2+ indicator traces of dsx-expressing neurons. X axis shows time; Y axis shows fluorescence intensity normalized to background signal. The red horizontal line represents the time and duration when red light was turned on for optogenetic activation. Quantification of these responses are shown on the right. Pink lines and dots show female samples, while blue dots show male samples. (E-F) Male (E) and female (F) Ca2+ indicator traces of dsx-expressing neurons upon a knockdown of sex-specific cell adhesion molecules in *DvPDF*-expressing neurons. Pink lines and dots represent knockdown of the female-enriched CAM, dpr3. Blue lines and dots represent knockdown of the male-enriched CAM, dpr9, in the LNds. Quantification of these responses are shown on the right. The red horizontal line represents the time and duration when light was turned on for optogenetic activation of *DvPDF*-expressing neurons.

Figure S1. Validation of sex-informed *de novo* cluster identification and sex-assignment cutoffs.

(A) Pearson's gene expression correlation heatmap between the newly generated sex-informed dataset and previously established circadian clusters from Ma et al., 2025. Numbers close to 1 show high correlation between the newly identified clusters and established cluster identity. (B) Normalized expression of *lncRNA:roX2* in sex-informed data set. Pink dots represent female-derived cells, blue dots show male-derived cells. (C) Normalized expression of *fru* in sex-informed data set. Pink dots represent female-derived cells, blue dots show male-derived cells. (D) Normalized expression of *Sxl* in sex-informed data set. Pink dots represent female derived cells; blue dots show male-derived cells. (E) Histogram plot of male and female derived cells against normalized *lncRNA:roX1* gene expression. Pink bars represent number of female cells; blue bars show the distribution of male cells with different *lncRNA:roX1* expression levels. (F) Log2 normalized *lncRNA:roX1* gene expression of male and female derived cells in sex-informed data set. Each dot represents a cell, pink violin shows female cells, blue violin show male cells. (G) AUROC plot used to determine optimal *lncRNA:roX1* expression cutoff based on sex-informed data set. X axis represents the false positive fraction; Y axis shows true positive fraction. Blue dot shows the optimal expression cutoff for calling a cell "male" (> 2.3) or "female" (< 2.3).

Figure S2. Validation of sex-assignment in sex-inferred dataset based on sex-informed cutoff.

(A) Histogram plot of male and female derived cells against normalized *lncRNA:roX1* gene expression. Pink bars represent number of inferred female cells; blue bars show the distribution of inferred male cells with different *lncRNA:roX1* expression levels. Grey bards show cells with undetermined sex based on stringent lncRNA:roX1 expression cutoffs. (B) Violin plot (normalized Log2 scale) of *lncRNA:roX1* gene expression of male and female derived cells in the sex-informed data set. Each dot represents a cell, pink violin shows female cells, blue violin show male cells. Grey violin show cells with undetermined sex based on stringent *lncRNA:roX1* expression cutoffs. (C) Number of cells per cluster separated by inferred sex. Pink bars show inferred female cells; blue bars show inferred male cells. Numbers represent the ratio of male to female neurons in the individual circadian clusters.

Figure S3. Remapping and reclustering previously published circadian single cell datasets.

(A) Percentage of lncRNAs expressed in the single-cell data set from Ma et al., 2025. The original dataset did not include lncRNAs (left violin plot). Remapped dataset to a genome containing lncRNA shows a higher percentage of cells expressing lncRNAs (right violin plots). (B) Dimensional reduction plot showing cluster identities of remapped dataset. (C) Dimensional reduction plot showing log2 normalized *lncRNA:roX1* expression distribution in remapped dataset. Green dashed circles show *roX1* biased clusters. (D) Pearson's gene expression correlation of published single cell dataset (Ma et al., 2025) and remapped dataset. Numbers closer to 1 reflect high cluster correlation indicating correct cluster identity assignment.

Figure S4. Validation of newly generated circadian neuron single cell dataset.

(A) Number of transcripts (nCount_RNA) and genes (nFeature_RNA) detected in the newly generated dataset for each single cell. (B) Number of high confidence circadian single cells recovered per timepoint across each circadian cell type. (C) Number of high confidence circadian single cells recovered per DGRP lines used across each circadian cell type. Two DGRP lines were used per timepoint representing biological replicates within a single experiment. (D) Validation of high confidence circadian clusters was done by cycling gene expression of core molecular clock components, *tim* (top) and *Clk* (bottom). X axis shows the timepoints collected in this new dataset. Y axis shows normalized TP10K expression for each individual cluster.

Figure S5. Marker gene expression in the sexually dimorphic clusters.

Log2 normalized gene expression of (A) *fru*, (B) *zld*, (C) *NPF*, and (D) *mGluR* in the circadian clusters. Dimorphic circadian clusters are shown on the left. Male-biased clusters are shown in blue, female-biased clusters are shown in pink. Clusters that show male and female co-clustering are shown in purple. *fru* is a defining feature of all clusters with dimorphic gene expression profile. *zld* is a defining feature of the dimorphic DN3 clusters (DN3-9a/d, DN3- 9c/b). *NPF* and *mGluR* are defining features of male LNds. Bracket indicates sexually dimorphic circadian cell types.

Figure S6. Sex-specific neural connectivity molecules within the DN3 dimorphic cell types.

(A) Violin plot showing (TP10K normalized scale) expression of neural connectivity molecules upregulated in either male (top) or female (bottom) DN3-9ad cells. CAMs (*kirre*), GPCRs (*AstC-R1, AstC-R2*, *mGluR* and *Oamb*) and neuropeptide (*sNPF*). (B) Violin plot showing (TP10K normalized scale) expression of neural connectivity molecules upregulated in either male (top) or female (bottom) DN3-9cb cells. CAMs (*DIP-eta*, *dpr9*, *Ten-a*, *dpr10*), and GPCRs (*AstC-R2* and *mGluR*).

Table 1. List of upregulated genes in male circadian cell types

LNd-1	DN3-9c	DN3-9a	DN1p-4	DN1p-6	DN2	DN1a, DN1p-5, DN3-1, DN3-2, DN3-4, DN3-7	DN1p-1, DN1p-2, DN1p-3	DN3-3, LPN-2	DN3-5	DN3-8	DN1p-7, DN3-6, DN3-10, DN3-12, LNd-3, LNvs, LPN-1
lncRNA:roX1	lncRNA:roX1	lncRNA:roX1	lncRNA:roX1	lncRNA:roX1	lncRNA:roX1	lncRNA:roX1	lncRNA:roX1	lncRNA:roX1	lncRNA:roX1	lncRNA:roX1	lncRNA:roX1
NPF	lncRNA:roX2	lncRNA:roX2	lncRNA:roX2	Proc	lncRNA:roX2	Muc14A	lncRNA:roX2	lncRNA:roX2	lncRNA:roX2	lncRNA:roX2	lncRNA:roX2
lncRNA:roX2	Nos	CG6959	Wnt4	lncRNA:roX2	Muc14A	lncRNA:roX2	trol	ssx	CG17777	lcs	
rgn	Scp2	CG14692	hid	HLH3B	trol						
CG43902	CG42342	CG3655	CG42674	Eip63E							
CG14340	DIP-eta	sNPF	Tbh	Xrp1							
Mp	Pde9	Muc14A	CG31176								
CG31221	CG6123	CG43658	pyd								
rdo	CG14692	Dop1R1	CG33543								
mGluR	dpr1	AstC-R2	nmo								
dpr9	CG18467	beat-IIIc	Dop1R2								
CG11317	dpr9	DIP-kappa	NetB								
CG42674	Sema2b	CG13054									
CG43373	sesB	Rgk3									
CG14431	Ggamma30A	CG9932									
CG34354	side-II	CG45002									
kek5	Pde11	nmo									
Rgk3	CG17839	AstC-R1									
Eip93F	side-IV	dpr1									
sca	rgn	Pde11									
ttv	oaf	CG17193									
dpr6	sky	Nlg3									
dpr16	Plc21C	Ppcs									
cpo	Ppcs	Stacl									
btsz	ssx	DIP-delta									
Ca-alpha1T	CG34370	dpr13									
Best1	AstC-R2	Cyt-c-p									
ssx	Trpm	Dh44									
Pde9	wake	CG30419									
Tdc2	Pura	ttv									
tna	hppy	dve									
rdgA	CG45002	Pde1c									
dpr12	CG4629	LpR1									
Octalpha2R	fz										
Hs3st-A	Muc14A										
CG11319											
CG42784											
Cngl											
CG15312											
Pxn											
Ddc											
igl											

Table 2. List of upregulated genes in female circadian cell types

DN3-9b	DN3-9d	LNd-2	DN1p-4	DN3-12	DN1p-2	DN2	DN3-1	DN3-5,DN3-7	DN1p-1	LNvs	LPN-2	DN1p-3	DN1p-6	DN1a, DN1p-5, DN1p-7, DN3-2, DN3-3, DN3-4, DN3-5, DN3-8, DN3-10, DN3-11, LPN1
Ten-a	CG15765	CG34353	CG34247	pre-rRNA:CR45845	CG42346	lncRNA:CR44997	CG15765	pre-rRNA:CR45845	Sxl	CG44422	Sxl	rk	CNMa	Sxl
CCAP-R	mGluR	Proc	CG15765	side-V	lncRNA:CR44997	Sxl	Sxl	Sxl	CG34247	Pdfr	CG42240	Sxl		
dpr10	CG32982	CG42394	pre-rRNA:CR45845	PVRAP	Sxl									
beat-IV	Ten-a	CG31705	Cbp53E	Ca-alpha1T										
Dgk	CG43373	lncRNA:CR44663	twit	Gyc32E										
CG15765	beat-Ic	dpr3	Sxl	Neto										
Sxl	Sxl	5-HT2B	Ggamma30A	Sxl										
CG32204	beat-Ib	pre-rRNA:CR45845	sca	CG42340										
CG44422	Oamb	ed	Osi4											
mGluR	kirre	CG43658	Fas2											
nAChRalpha7	alpha-Man-Ia	CG13950	CG43078											
B4	rst	alpha-Man-Ia	CG34357											
PVRAP	dnc	Fkbp14	RYa-R											
CG17716	CG44422	CG12541	Gprk2											
side-VIII	Invadolysin	CG44837	mamo											
Rbp6	CG11000	Myc	sNPF											
tutl	mgl	Pde6	MsR1											
beat-VI	eys	CG15765												
CG18599	Rh7	Pdfr												
ed	igl													
kirre	app													
FER	CG33639													
DIP-zeta	CG32204													
Fili	side-VIII													
Fas2	Dscam3													
mbl	SKIP													
dnc	CG17716													
CG13229	CBP													
Pdfr	beat-VII													
CG42402	mAChR-B													
l(3)neo38	PVRAP													
pre-rRNA:CR45845														

Table S1. List of fly strains used for single-cell RNA-seq and behavior experiments

Genotype	Source	Stock number
CLK856-Gal4	Bloomington Drosophila Stock Center	BDSC 93198
DN3-splitGal4	Ma et al. 2025	NA
UAS-eGFP	Bloomington Drosophila Stock Center	BDSC 5430
UAS-Cas9.P2 (attP40)	Bloomington Drosophila Stock Center	BDSC 58985
UAS-Cas9.P2 (attP2	Bloomington Drosophila Stock Center	BDSC 58986
DvPDF-Gal4	Bahn et al., 2009	NA
Clk21-Gal4	Gift from Paul Hardin	NA
UAS-3Xg-fru	This study	NA
UAS-3Xg-NPF	This study	NA
UAS-3Xg-Proc	This study	NA
UAS-3Xg-mGluR	Schlichting et al., 2019	BDSC 97808
UAS-3Xg-5HT2B	Schlichting et al., 2019	BDSC 97760
UAS-3Xg-dpr9	This study	NA
UAS-3Xg-dpr3	This study	NA
nsyb-GRASP	Bloomington Drosophila Stock Center	BDSC 64314

Table S2. List of primers used to generate guide RNA fly lines

Name	Sequence 5' to 3'
fru-1	CGGCCCGGGTTCGATTCCCGGCCGATGCA**CCAGTTCGCCGACCGGACGT**GTTTCAGAGCTATGCTGGAAAC
fru-2	**GTTTTGGGCACGGGACTCGA**TGCACCAGCCGGGAATCGAACC
fru-3	**TCGAGTCCCGTGCCCAAAAC**GTTTCAGAGCTATGCTGGAAAC
fru-4	ATTTTAACTTGCTATTTCTAGCTCTAAAAC**TACTTCGAGACGATTTTCCT**TGCACCAGCCGGGAATCGAACC
NPF-1	GGCCCGGGTTCGATTCCCGGCCGATGCA**CCAAACAATGCGTTGCATCC**GTTTCAGAGCTATGCTGGAAAC
NPF-2	**CACAGGCAACCAGGATGCAA**TGCACCAGCCGGGAATCGAACC
NPF-3	**TTGCATCCTGGTTGCCTGTG**GTTTCAGAGCTATGCTGGAAAC
NPF-4	TTTAACTTGCTATTTCTAGCTCTAAAAC**GTGTGGCCCTTGCCCTCCTA**TGCACCAGCCGGGAATCGAACC
Proc-1	CGGCCCGGGTTCGATTCCCGGCCGATGCA**GGCGGAGATGGAGCCCGGTT**GTTTCAGAGCTATGCTGGAAAC
Proc-2	**CGCGTGTCCAACGGCAACTC**TGCACCAGCCGGGAATCGAACC
Proc-3	**GAGTTGCCGTTGGACACGCG**GTTTCAGAGCTATGCTGGAAAC
Proc-4	ATTTTAACTTGCTATTTCTAGCTCTAAAAC**TTGGACACGCGTGGATTGTT**TGCACCAGCCGGGAATCGAACC
dpr9-1	GGCCCGGGTTCGATTCCCGGCCGATGCA**TCCCACTCCTTCGTTGGGCA**GTTTCAGAGCTATGCTGGAAAC
dpr9-2	**TCCGCTTCCGTCGATACCAG**TGCACCAGCCGGGAATCGAACC
dpr9-3	**CTGGTATCGACGGAAGCGGA**GTTTCAGAGCTATGCTGGAAAC
dpr9-4	TTTAACTTGCTATTTCTAGCTCTAAAAC**TGCGTGATTGTGGCTTCAGA**TGCACCAGCCGGGAATCGAACC
dpr3-1	CGGCCCGGGTTCGATTCCCGGCCGATGCA**ACAGGAATGTCGACAGGGTT**GTTTCAGAGCTATGCTGGAAAC
dpr3-2	**AGGGATCCCCGAGGACACGT**TGCACCAGCCGGGAATCGAACC
dpr3-3	**ACGTGTCCTCGGGGATCCCT**GTTTCAGAGCTATGCTGGAAAC
dpr3-4	ATTTTAACTTGCTATTTCTAGCTCTAAAAC**GATGACTCCGGTGATGGCCC**TGCACCAGCCGGGAATCGAACC